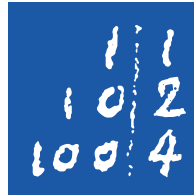
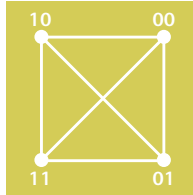


Institut für
Kommunikations-
Technik



Leibniz
Universität
Hannover

On the Effect of Shadow Fading on Wireless Geolocation in Mixed LoS/NLoS Environments

Bamrung Tau Sieskul, Feng Zheng, and Thomas Kaiser

IEEE Transactions on Signal Processing, vol. 57, no. 11, pp. 4196-4208, Nov. 2009.

Copyright (c) 2009 IEEE. Personal use of this material is permitted. However, permission to use this material for any other purposes must be obtained from the IEEE by sending a request to pubs-permissions@ieee.org.

On the Effect of Shadow Fading on Wireless Geolocation in Mixed LoS/NLoS Environments

Bamrung Tau Sieskul, *Student Member, IEEE*, Feng Zheng, *Senior Member, IEEE*, and Thomas Kaiser, *Senior Member, IEEE*

Abstract—This paper considers the wireless non-line-of-sight (NLoS) geolocation in mixed LoS/NLoS environments by using the information of time-of-arrival. We derive the Cramér–Rao bound (CRB) for a deterministic shadowing, the asymptotic CRB (ACRB) based on the statistical average of a random shadowing, a generalization of the modified CRB (MCRB) called a simplified Bayesian CRB (SBCRB), and the Bayesian CRB (BCRB) when the *a priori* knowledge of the shadowing probability density function is available. In the deterministic case, numerical examples show that for the effective bandwidth in the order of kHz, the CRB almost does not change with the additional length of the NLoS path except for a small interval of the length, in which the CRB changes dramatically. For the effective bandwidth in the order of MHz, the CRB decreases monotonously with the additional length of the NLoS path and finally converges to a constant as the additional length of the NLoS path approaches the infinity. In the random shadowing scenario, the shadowing exponent is modeled by $\zeta = u\sigma$, where u is a Gaussian random variable with zero mean and unit variance and σ is another Gaussian random variable with mean μ_σ and standard deviation σ_σ . When μ_σ is large, the ACRB considerably increases with σ_σ , whereas the SBCRB gradually decreases with σ_σ . In addition, the SBCRB can well approximate the BCRB.

Index Terms—Non-line-of-sight propagation, parameter estimation, shadowing effect.

I. INTRODUCTION

WIRELESS geolocation commercially emerges from the incentives of locating vehicle, people and parcels (see, e.g., [1]–[3]). Promising applications encompass accident reporting, navigational services, automated billing, fraud detection, roadside assistance, and cargo tracking. For wireless carriers and vendors, the knowledge of a user position leads to more charge precision and service plans. In cellular systems, the problem of finding the position of mobile stations (MSs) can be accomplished using the measurements of a mobile signal at multiple base stations (BSs) [4]. Invoking the information of time of arrival (ToA) can provide an accurate estimate for the distance between the transmitter and the receiver. The line-of-sight (LoS) distances between a mobile and at least three participating BSs

are observed to locate the mobile terminal in a two dimensional space.

In [5], the analysis of non-line-of-sight (NLoS) geolocation is unified where no NLoS mitigation is accounted for and the additional NLoS path length is assumed to be unknown. It is shown that the Cramér–Rao bound (CRB) is independent of the NLoS when the shadowing is unknown. For the environment where some or all measuring distances are subject to the LoS, a residual test is presented to determine the number of LOS measurements and the position is estimated from the determined LoS measurement [6]. Contrary to the LoS restriction, the NLoS paths in a direction-based system are exploited to improve the positioning accuracy [7]. When the *a priori* knowledge of an NLoS-induced error is available, the best geolocation accuracy is derived in term of a generalized CRB [5], which is actually the Bayesian CRB (BCRB) in the classical terminology [8]. Furthermore, the ToA performance is analyzed therein without taking path attenuation into account, which significantly affects the received power [9]. From these previous results, a further investigation on the localization problem for other scenarios is necessary.

In this paper, we address the inherent accuracy limitation for the problem of estimating a mobile position based on multi-lateral ToA measurements in the presence of shadow fading. This problem is deemed important, because it more realistically reflects the system model in the wireless geolocation problem based on the ToA information. The path amplitude is modeled by a lognormal-distributed shadowing, which heuristically can be characterized by a multiplicative process [10]. In the path loss model, we assume that the environment is located in a suburban area where the propagations between the MS and BSs do not switch rapidly from the LoS to the NLoS or vice versa. We derive the CRB in the continuous time for the case of deterministic shadowing, and the asymptotic CRB (ACRB) in a statistical average sense, a generalization of the modified CRB (MCRB) introduced in [11] and called herein the simplified BCRB (SBCRB), and the BCRB for the random shadowing case.

The research gap among this work and the previous works is that most former works consider the path gain in the wireless NLoS geolocation as an unstructured quantity, but in this work, more features of a wireless channel are considered. Precisely, the path gain is decomposed into two large-scale fading. The first large-scale fading captures a path loss model, while the second large-scale fading represents the shadowing. We assume that the large-scale fading can be considered as a spatial average over the small-scale fluctuations of the signals [12, p. 847].

The contribution of this paper can be described twofold. First, we present a framework for the geolocation problem taking both

Manuscript received December 20, 2007; accepted May 05, 2009. First published June 10, 2009; current version published October 14, 2009. The associate editor coordinating the review of this manuscript and approving it for publication was Dr. Mats Bengtsson.

The authors are with the Institute of Communications Technology, Faculty of Electrical Engineering and Computer Science, Leibniz University of Hannover, 30167 Hannover, Germany (e-mail: bamrung.tausieskul@ikt.uni-hannover.de; feng.zheng@ikt.uni-hannover.de; thomas.kaiser@ikt.uni-hannover.de).

Color versions of one or more of the figures in this paper are available online at <http://ieeexplore.ieee.org>.

Digital Object Identifier 10.1109/TSP.2009.2025084

the path loss and the shadowing into account. Second, we provide the performance bounds for the geolocation problem of two scenarios depending on whether the shadowing is fixed or random. For the random shadowing case, the bound is averaged over all the realizations of the shadowing. In addition, when the distribution of the shadowing is known *a priori*, we provide a pseudo performance bound, which is computationally inexpensive and can well approximate the exact and complicated one.

The rest of this paper is organized as follows. In Section II, the transceiver model of the wireless NLoS geolocation is reviewed. In Section III, we derive a closed form of the CRB when the shadow fading is assumed deterministic. In Section IV, the case of the random shadow fading is discussed as well as the ACRB, the SBCRB and the BCRB are presented. In Section V, numerical examples are provided to illustrate the effects of the shadow fading on the performance bound of the range estimation in the wireless NLoS geolocation. In Section VI, the conclusions are drawn.

In the sequel, $(\cdot)^T$ denotes the transpose of a matrix. $\|\cdot\|_E$ is the Euclidean norm. The notation $x \sim \mathcal{N}(\mu, \sigma^2)$ means that the real random variable x is distributed (real) normal with the probability density function (PDF) $f_x(x) = (1/\sqrt{2\pi}\sigma)e^{-(1/2)(x-\mu)^2/\sigma^2}$. The notation $x \sim \mathcal{N}_C(\mu, \sigma^2)$ means that the complex random variable x is distributed (complex) normal with the PDF $f_x(x) = (1/\pi\sigma^2)e^{-|x-\mu|^2/\sigma^2}$. The operator \odot stands for the (element-wise) Hadamard product. The expectation $E_{\hat{\theta}}\{\cdot\}$ is performed with respect to $\hat{\theta}$. The inverse of a matrix is denoted by $(\cdot)^{-1}$. $\mathbf{B} \succeq \mathbf{C}$ means that the matrix $\mathbf{B} - \mathbf{C}$ is positive semi-definite. The trace of a square matrix is denoted by $\text{tr}(\cdot)$. The functional matrix $\mathbf{D}(\cdot)$ is the diagonal matrix whose diagonal vector is taken from the vector \cdot . The column vector $\mathbf{1}_M$ is of M dimensions, where each entry is one.

II. SYSTEM MODEL

Consider an MS transmitting a radio signal through a wireless channel to a number of the BSs. Let B be the number of all BSs, whose locations, $\mathbf{p}_b = [x_b \ y_b]^T$, $b \in \{1, 2, \dots, B\}$, are known. We assume that there is attenuation in the channel and no additional loss of energy is taken into account in the wave propagation. At the b th BS, the received energy can be expressed by [13]

$$E_b = \frac{d_0^{\gamma_b}}{d_b^{\gamma_b}} \kappa \xi_b E_s \quad (1)$$

where d_0 is the close-in reference in the far field region, d_b is the distance between the MS and the b th BS, γ_b is the path loss exponent at the b th BS, $E_s = \int_{-\infty}^{\infty} |s(t)|^2 dt$ is the energy of transmit signal $s(t)$, $\xi_b = 10^{(1/10)\zeta_b}$ is the shadow fading with the shadowing exponent ζ_b , and the unitless constant¹ κ depending on antenna characteristics and average channel attenuation is given by

$$\kappa = \frac{c^2}{16\pi^2 f_0^2 d_0^2} \quad (2)$$

¹The constant κ appears as a free-space path loss at the reference distance d_0 . In fact, the choice of d_0 could depend on the antenna characteristics.

with the central frequency of the wireless system f_0 and the speed of light c . At $f_0 = 1.9$ GHz and for $d_0 = 100$ m, it is shown in [13] that $\kappa_{\text{dB}} = 10 \log_{10} \kappa \simeq -78$ dB. We assume that the LoS/NLoS detection has already been performed and consider the case that the NLoS error correction is not conducted². Let $M < B - 1$ be the number of the BSs that receive a set $\{1, 2, \dots, M\}$ of NLoS signals. It is further assumed that the number M is known. The received signal amplitude, denoted by α_b ; $b \in \{1, 2, \dots, B\}$, and the additional distance induced by the NLoS, denoted by l_m ; $m \in \{1, 2, \dots, M\}$, are assumed to be unknown, whereas the position of the MS, $\mathbf{p} = [x \ y]^T$, is the parameter of interest. Let τ_b be the time delay of the received signal at the b th BS given by

$$\tau_b(x, y, l_b) = \begin{cases} \frac{1}{c} \left(\sqrt{\tilde{x}_b^2 + \tilde{y}_b^2} + l_b \right); & b \in \{1, \dots, M\}, \\ \frac{1}{c} \sqrt{\tilde{x}_b^2 + \tilde{y}_b^2}; & b \in \{M+1, \dots, B\} \end{cases} \quad (3)$$

where $\tilde{x}_b = x - x_b$, $\tilde{y}_b = y - y_b$, and $l_b = 0$; for $b \in \{M+1, M+2, \dots, B\}$. It should be noted that in (3), only a single NLoS path between the receiver and the transmitter is taken into account. This assumption is justifiable for the geolocation problem since only the first path is necessary for extracting the position. As $d_b = c\tau_b$, the noiseless energy based on (1) can be rewritten as

$$E_b = \kappa \left(\frac{d_0}{\sqrt{\tilde{x}_b^2 + \tilde{y}_b^2} + l_b} \right)^{\gamma_b} \xi_b E_s. \quad (4)$$

Since (1) and (4) are valid only in the far field, it is assumed that d_0 is less than $\sqrt{\tilde{x}_b^2 + \tilde{y}_b^2}$. It means that there is no BS within the circle of the radius d_0 .

In general, the shadowing is a slow fading whose variation period is larger than the coherence time, i.e., the period over which the fading process is correlated. Herein, we assume that the signal bandwidth is smaller than the coherence bandwidth so that the channel is frequency flat. The received baseband signal can be written as³ [5]

$$r_b(t) = \alpha_b s(t - \tau_b) + n_b(t); \quad b \in \{1, 2, \dots, B\} \quad (5)$$

where $s(t)$ is the signal waveform, α_b and τ_b are the amplitude and the time delay of the propagation to the b th BS, and $n_b(t)$ is the additive noise at the b th BS and assumed to be a complex-valued white Gaussian random process with the spectral density $(1/2)N_0$. In (5), the waveform of the signal $s(t)$ is assumed to be known at the receivers and this assumption is used throughout the paper. Furthermore, we assume the perfect time synchronization between the transmitter and the receiver so that there is no further mismatched time delay other than the propagation delay τ_b . In the next section, we assume that the position \mathbf{p} and the nuisance parameters l_b and ξ_b are unknown and deterministic. So is the reparameterized time delay τ_b . To make the model tractable, we assume that channel parameters from

²The NLoS can be mitigated using the method in e.g., [14].

³Since we assume a single path, the effects of small-scale fading are ignored, and only shadow fading is studied. Therefore, the results presented in this paper does not apply to the case of multipath propagation, since the distributions of the signal amplitude will be likely different from that adopted in this paper due to the small-scale fading. However, the method outlined in this paper can be extended to the case of multipath propagation to obtain similar results.

all BSs are identical, i.e., $\gamma_b = \gamma$ and $\xi_b = \xi$ for all b . For different fading at the BS receivers, the analysis can be conducted in the same way⁴. Since $E_b = \alpha_b^2 E_s$, the parameter α_b is given by

$$\alpha_b = \sqrt{\kappa} \left(\frac{d_0}{\sqrt{\tilde{x}_b^2 + \tilde{y}_b^2 + l_b}} \right)^{(1/2)\gamma} \sqrt{\xi}. \quad (6)$$

Note that when there is no path attenuation and no shadow fading ($\gamma_b = 0$ and $\xi = 1$), the amplitude becomes $\alpha_b = \sqrt{\kappa} = c/4\pi f d_0$. In a vector form, the received signal in (5) can be written as

$$\mathbf{r}(t) = \boldsymbol{\alpha}(\boldsymbol{\tau}, \xi) \odot \mathbf{s}(t, \boldsymbol{\tau}) + \mathbf{n}(t) \quad (7)$$

where $\mathbf{r}(t) \in \mathbb{C}^{B \times 1}$, $\boldsymbol{\alpha} \in \mathbb{R}_+^{B \times 1}$, $\mathbf{s}(t) \in \mathbb{C}^{B \times 1}$, $\boldsymbol{\tau} \in \mathbb{R}_+^{B \times 1}$, and $\mathbf{n}(t) \in \mathbb{C}^{B \times 1}$ are defined by

$$\mathbf{r}(t) = [r_1(t) \ r_2(t) \ \cdots \ r_B(t)]^T \quad (8a)$$

$$\boldsymbol{\alpha} = [\alpha_1 \ \alpha_2 \ \cdots \ \alpha_B]^T \quad (8b)$$

$$\mathbf{s}(t, \boldsymbol{\tau}) = [s_1(t-\tau_1) \ s_2(t-\tau_2) \ \cdots \ s_B(t-\tau_B)]^T \quad (8c)$$

$$\boldsymbol{\tau} = [\tau_1 \ \tau_2 \ \cdots \ \tau_B]^T \quad (8d)$$

$$\mathbf{n}(t) = [n_1(t) \ n_2(t) \ \cdots \ n_B(t)]^T. \quad (8e)$$

Assume that the transmitted signal is nonzero over the interval $(0, T_s]$ and also band-limited to 2β Hz, where T_s is a signal period. Afterwards, the signal is passed onto an ideal bandpass filter in order to get rid of the noise outside of the frequency band $[-\beta, \beta]$. Note that the noise variance is $\sigma_n^2 = N_0\beta$. Let us define the signal-to-noise ratio (SNR) at the transmitter as

$$\text{SNR} = \frac{E_s}{N_0} = \frac{1}{N_0} \int_0^{T_s} |s(t)|^2 dt \quad (9)$$

and the effective (root-mean-square) bandwidth $\bar{\beta}$ as [15, eq. (9)]

$$\bar{\beta} = 2\pi \sqrt{\frac{\int_{-\infty}^{\infty} f^2 |S(f)|^2 df}{\int_{-\infty}^{\infty} |S(f)|^2 df}} \quad (10)$$

where $S(f)$ is the Fourier transform of the signal $s(t)$. The received SNR⁵ is given by $\widetilde{\text{SNR}}_b = \alpha_b^2 \text{SNR}$. Note that for the NLoS BSs, the gain $\widetilde{\text{SNR}}_b/\text{SNR}$ is a decreasing function of the additional NLoS path length l_b , i.e., $\widetilde{\text{SNR}}_b/\text{SNR} \propto 1/\left(\sqrt{\tilde{x}_b^2 + \tilde{y}_b^2 + l_b}\right)^\gamma$.

⁴For instance, we may assume that there exists shadowing only at the NLoS BSs and the shadowing can be different among the NLoS BSs. Then, there can be maximal M unknown shadowing coefficients, whereas the model is still identifiable if $B > 2M + 2$.

⁵When considering the path attenuation such as in this paper, the received SNR is related to parameter α_b , which depends on several parameters including κ (which again depends on d_0 and f_0), d_b , γ , and ξ . Since the effects of these parameters on the geolocation performance will be investigated in this paper, we need to adjust the value of these parameters. In this case, it is inconvenient to set the received SNR at a specific value. Therefore, in the simulations, we consider the transmitted SNR, which is defined as the ratio between the transmitted power and the noise power at the receiver, rather than the received SNR.

III. DETERMINISTIC SHADOWING

In this section, we assume that the observation period is equal to the symbol period, which is less than the coherence time. It means that in one observation period, the shadowing stays constant. In this case, the shadow fading ξ can be considered deterministic. All the unknown parameters can be aggregated into the vector $\boldsymbol{\theta} \in \mathbb{R}^{(M+3) \times 1}$ as

$$\boldsymbol{\theta} = [\mathbf{p}^T \ \mathbf{l}^T \ \xi]^T \quad (11)$$

where $\mathbf{p} \in \mathbb{R}^{2 \times 1}$ and $\mathbf{l} \in \mathbb{R}_+^{M \times 1}$ are given by

$$\mathbf{p} = [x \ y]^T \quad (12a)$$

$$\mathbf{l} = [l_1 \ l_2 \ \cdots \ l_M]^T. \quad (12b)$$

The received signal is distributed as $r_b(t) \sim \mathcal{N}_C(\alpha_b s(t - \tau_b), \sigma_n^2)$. When all BSs are far apart enough from each other, the received signals from all BSs can be assumed mutually independent. The joint PDF of $r_1(t), \dots, r_B(t)$ can be written as

$$\begin{aligned} f_{\mathbf{r}(t)}(\mathbf{r}(t)) &= \prod_{b=1}^B f_{r_b(t)}(r_b(t)) \\ &= \frac{1}{(\pi\sigma_n^2)^B} e^{-(1/\sigma_n^2)\|\mathbf{r}(t) - \boldsymbol{\alpha} \odot \mathbf{s}(t, \boldsymbol{\tau})\|_E^2}. \end{aligned} \quad (13)$$

At the receiver, the continuous received waveform is sampled at the Nyquist sampling period of $\delta = 1/2\beta$ seconds to form the observation data

$$r_b(n\delta) = a_b s(n\delta - \tau_b) + n_b(n\delta); \quad n \in \{0, 1, \dots, N-1\} \quad (14)$$

where N is the number of samples. Here the interval of interest lies in such a way that $\boldsymbol{\theta}$ is invariant in $(0, (N-1)\delta]$. If $r_b[n]$, $s[n; \tau_b]$ and $n_b[n]$ are the sampled sequences, the discrete data model can be written as

$$r_b[n] = a_b s[n; \tau_b] + n_b[n]. \quad (15)$$

Note that the signal is nonzero only over the interval $\tau_b \leq t \leq \tau_b + T_s$. Then, the received signal becomes [16, p. 54]

$$r_b[n] = \begin{cases} n_b[n] & 0 \leq n \leq \eta_b - 1 \\ a_b s[n\delta; \tau_b] + n_b[n] & \eta_b \leq n \leq \eta_b + N_s - 1 \\ n_b[n] & \eta_b + N_s \leq n \leq N - 1 \end{cases} \quad (16)$$

where N_s is the length of the sampled signal and $\eta_b = \tau_b/\delta$ is the delay in samples. Define

$$\mathbf{r}[n] = [r_1[n] \ r_2[n] \ \cdots \ r_B[n]]^T \quad (17a)$$

$$\mathbf{s}[n; \boldsymbol{\tau}] = [s[n; \tau_1] \ s[n; \tau_2] \ \cdots \ s[n; \tau_B]]^T \quad (17b)$$

$$\mathbf{n}[n] = [n_1[n] \ n_2[n] \ \cdots \ n_B[n]]^T. \quad (17c)$$

It follows that

$$\mathbf{r}[n] = \boldsymbol{\alpha}(\boldsymbol{\tau}, \xi) \odot \mathbf{s}[n; \boldsymbol{\tau}] + \mathbf{n}[n]. \quad (18)$$

Since the measurement noise is white, the received signals at different time instants are independent of each other. Therefore,

the PDF of the observation \mathbf{r} over the period $(0, T_o]$, $f_{\mathbf{r}|\boldsymbol{\theta}}(\mathbf{r}|\boldsymbol{\theta}) = \lim_{\delta \rightarrow 0} \prod_{n=0}^{T_o/\delta} f_{\mathbf{r}[n]}(\mathbf{r}[n])$, is given by (19) shown at the bottom of the page, where $T_o = (N - 1)\delta$, which is larger than $T_s = (N_s - 1)\delta$, is the observation period, and $\tilde{\mathbf{s}}(t; \boldsymbol{\tau}, \xi)$ is defined by $\tilde{\mathbf{s}}(t; \boldsymbol{\tau}, \xi) = \boldsymbol{\alpha}(\boldsymbol{\tau}, \xi) \odot \mathbf{s}(t, \boldsymbol{\tau})$. The log-likelihood function is given by

$$\ln(f_{\mathbf{r}|\boldsymbol{\theta}}(\mathbf{r}|\boldsymbol{\theta})) = -2BT_o\beta(\ln(\pi) + \ln(N_o) + \ln(\beta)) - \frac{1}{N_o} 2 \int_0^{T_o} \|\mathbf{r}(t) - \tilde{\mathbf{s}}(t; \boldsymbol{\tau}, \xi)\|_{\mathbb{E}}^2 dt. \quad (20)$$

A. Cramér–Rao Bound

Let $\hat{\boldsymbol{\theta}}$ be any unbiased estimate of $\boldsymbol{\theta}$ based on the measurement of (5). Then, the accuracy of $\hat{\boldsymbol{\theta}}$ is bounded according to the Cramér–Rao inequality

$$\mathbb{E}_{\hat{\boldsymbol{\theta}}} \{(\hat{\boldsymbol{\theta}} - \boldsymbol{\theta})(\hat{\boldsymbol{\theta}} - \boldsymbol{\theta})^T\} \succeq \mathbf{H}_{\boldsymbol{\theta}\boldsymbol{\theta}}^{-1} \quad (21)$$

where $\mathbf{H}_{\boldsymbol{\theta}\boldsymbol{\theta}} \in \mathbb{R}^{(M+3) \times (M+3)}$ is the Fisher information matrix (FIM) derived from [16]

$$\mathbf{H}_{\boldsymbol{\theta}\boldsymbol{\theta}} = -\mathbb{E}_{\mathbf{r}} \left\{ \frac{\partial^2}{\partial \boldsymbol{\theta} \partial \boldsymbol{\theta}^T} \ln(f_{\mathbf{r}|\boldsymbol{\theta}}(\mathbf{r}|\boldsymbol{\theta})) \right\}. \quad (22)$$

Proposition 1 (Deterministic CRB): The CRB of the mobile position estimate, $\mathbf{B}_{\mathbf{p}} \in \mathbb{R}^{2 \times 2}$ computed from the block inverse of $\mathbf{H}_{\boldsymbol{\theta}\boldsymbol{\theta}}$, is given by

$$\mathbf{B}_{\mathbf{p}} = \frac{4\pi^2 f^2}{d_0^{\gamma-2} \text{SNR} \beta^2 \xi} (\bar{\boldsymbol{\Phi}} \mathbf{A}(\varrho) \bar{\boldsymbol{\Phi}}^T)^{-1} \quad (23)$$

where $\mathbf{A}(\varrho) \in \mathbb{R}^{(B-M) \times (B-M)}$ is defined by

$$\begin{aligned} \mathbf{A}(\varrho) &= \mathbf{D}^{-(1/2)\gamma}(\bar{\mathbf{d}}) \left(\mathbf{I}_{(B-M)} + \frac{1}{4\beta^2} c^2 \gamma^2 \mathbf{D}^{-1}(\bar{\mathbf{d}}) \right. \\ &\quad \left(\mathbf{I}_{(B-M)} - \mathbf{D}^{-(1/2)\gamma}(\bar{\mathbf{d}}) \boldsymbol{\Psi}(\varrho) \mathbf{D}^{-(1/2)\gamma}(\bar{\mathbf{d}}) \right. \\ &\quad \left. \left. \mathbf{D}^{-1}(\bar{\mathbf{d}}) \right) \mathbf{D}^{-(1/2)\gamma}(\bar{\mathbf{d}}) \right) \end{aligned} \quad (24)$$

with $\bar{\boldsymbol{\Phi}} \in \mathbb{R}^{2 \times (B-M)}$ given by

$$\bar{\boldsymbol{\Phi}} = \begin{bmatrix} \cos(\phi_{M+1}) & \cos(\phi_{M+2}) & \cdots & \cos(\phi_B) \\ \sin(\phi_{M+1}) & \sin(\phi_{M+2}) & \cdots & \sin(\phi_B) \end{bmatrix} \quad (25)$$

with ϕ_b derived from

$$\phi_b = \arctan \left(\frac{y - y_b}{x - x_b} \right) \quad (26)$$

with $\boldsymbol{\Psi}(\varrho) \in \mathbb{R}^{(B-M) \times (B-M)}$ given by

$$\boldsymbol{\Psi}(\varrho) = \frac{1}{\varrho} \mathbf{1}_{B-M} \mathbf{1}_{B-M}^T \quad (27)$$

with ϱ derived from

$$\begin{aligned} \varrho &= \mathbf{1}_{B-M}^T \mathbf{D}^{-\gamma}(\bar{\mathbf{d}}) \mathbf{1}_{B-M} - \frac{1}{4\beta^2} c^2 \gamma^2 \mathbf{1}_M^T \mathbf{D}^{-(\gamma+2)}(\tilde{\mathbf{d}}) \mathbf{1}_M \\ &= \sum_{b=M+1}^B \frac{1}{(\sqrt{\tilde{x}_b^2 + \tilde{y}_b^2})^\gamma} - \frac{1}{4\beta^2} c^2 \gamma^2 \sum_{b=1}^M \frac{1}{(\sqrt{\tilde{x}_b^2 + \tilde{y}_b^2 + l_b})^{\gamma+2}} \end{aligned} \quad (28)$$

and $\tilde{\mathbf{d}} \in \mathbb{R}^{M \times 1}$ and $\bar{\mathbf{d}} \in \mathbb{R}^{(B-M) \times 1}$ given by

$$\tilde{\mathbf{d}} = [d_1 \quad d_2 \quad \cdots \quad d_M]^T \quad (29a)$$

$$\bar{\mathbf{d}} = [d_{M+1} \quad d_{M+2} \quad \cdots \quad d_B]^T. \quad (29b)$$

Proof: See the Appendix. \blacksquare

At the critical point of $\bar{\beta}$ such that $\varrho = 0$, we can see from (86) that the Schur complement ρ in (81) is also zero. It means that the joint estimation of the shadowing amplitude ξ and the time delay $\boldsymbol{\tau}$ is impossible. It follows from (83) that the estimation of the mobile position \mathbf{p} is also infeasible. Define

$$\bar{\beta}_c = \frac{1}{2} c \gamma \sqrt{\frac{\sum_{b=1}^M \frac{1}{(\sqrt{\tilde{x}_b^2 + \tilde{y}_b^2 + l_b})^{\gamma+2}}}{\sum_{b=M+1}^B \frac{1}{(\sqrt{\tilde{x}_b^2 + \tilde{y}_b^2})^\gamma}}}. \quad (30)$$

From (28), it can be seen that the wireless NLoS geolocation cannot be performed when $\bar{\beta} = \bar{\beta}_c$. It is clear that the critical value of the effective bandwidth, $\bar{\beta}_c$, is a decreasing function of the additional length of the NLoS paths. If the MS transmits the signal with the effective bandwidth larger than the critical value $\bar{\beta}_c$, ϱ is positive and then the CRB will decrease with the increase of the excess NLoS path length. If the transmitted signal possesses a less effective bandwidth than the critical value $\bar{\beta}_c$, ϱ is negative and then the CRB decreases as the additional length of the NLoS path increases. In general, $\bar{\beta}_c$ is influenced by the power decay exponent γ and the positions of the BSs.

$$\begin{aligned} f_{\mathbf{r}|\boldsymbol{\theta}}(\mathbf{r}|\boldsymbol{\theta}) &= \lim_{\delta \rightarrow 0} e^{-B \ln(\pi \sigma_n^2)(1/\delta) \int_0^{T_o} dt - (1/\sigma_n^2)(1/\delta) \int_0^{T_o} \|\mathbf{r}(t) - \tilde{\mathbf{s}}(t; \boldsymbol{\tau}, \xi)\|_{\mathbb{E}}^2 dt} \\ &= e^{-B \ln(\pi(N_o \beta))(1/(1/2\beta)) \int_0^{T_o} dt - (1/N_o \beta)(1/(1/2\beta)) \int_0^{T_o} \|\mathbf{r}(t) - \tilde{\mathbf{s}}(t; \boldsymbol{\tau}, \xi)\|_{\mathbb{E}}^2 dt} \\ &= e^{-2BT_o \beta (\ln(\pi) + \ln(N_o) + \ln(\beta)) - (1/N_o) 2 \int_0^{T_o} \|\mathbf{r}(t) - \tilde{\mathbf{s}}(t; \boldsymbol{\tau}, \xi)\|_{\mathbb{E}}^2 dt}, \end{aligned} \quad (19)$$

B. Inherent Accuracy Behavior

The CRB in (23) is explicitly shown as a deterministic function of the shadow fading ξ . We can see that when the shadow fading ξ is larger, the accuracy of the mobile position estimate is higher⁶. The shadow fading ξ behaves in the same manner as the SNR, due to its scaling nature. When the additional path length of the NLoS is larger, the CRB becomes lower. This is because when $d_b = \sqrt{x_b^2 + y_b^2} + l_b$, $b \in \{1, 2, \dots, M\}$, is larger, ϱ is also larger. As a consequence, $\Psi(\varrho)$ becomes smaller and thus \mathbf{B}_p is smaller. For the extreme case, where $l_b \rightarrow \infty$, it can be observed that $\lim_{l_b \rightarrow \infty} \varrho = \mathbf{1}_{B-M}^T \mathbf{D}^{-\gamma}(\bar{\mathbf{d}}) \mathbf{1}_{B-M}$. It follows that the bound derived above converges to a value as the additional path length of the NLoS approaches the infinity.

IV. RANDOM SHADOWING

In the wireless geolocation, the training period may consist of several symbol periods during which the shadowing changes randomly. Therefore, we need to investigate the case where the shadowing parameter is a random variable. In this section, the shadow fading is modeled by

$$\tilde{\xi} = 10^{(1/10)\zeta} = e^{\nu\zeta} \quad (31)$$

where $\nu = (1/10) \ln(10)$ is a constant, and ζ is the shadowing exponent. The purpose of this modeling is to investigate how the random shadowing affects the wireless NLoS geolocation. The contribution in what follows is that the performance of the wireless NLoS geolocation is quantified in term of the CRB variants conditioned on the knowledge of the shadowing distribution available at the BSs. Let ε_{CRB} be the CRB in Proposition 1 for the estimate of the mobile position in both axes, i.e.,

$$\varepsilon_{\text{CRB}}(\zeta) = \sqrt{\text{tr}(\mathbf{B}_p(\zeta))}. \quad (32)$$

In the deterministic model, the shadowing effect on the NLoS geolocation can be evaluated by

$$\varepsilon = \frac{\varepsilon_{\text{CRB}}(\zeta)}{\varepsilon_{\text{CRB}}(\zeta = 0)} = e^{-(1/2)\nu\zeta}. \quad (33)$$

In general, the shadowing exponent ζ is considered random. The shadowing exponent ζ can be expressed as [13]

$$\zeta = u\sigma \quad (34)$$

where σ is the standard deviation of ζ , and u is a Gaussian random variable with zero mean and unit standard deviation. The standard deviation of ζ can be further modeled as $\sigma \sim \mathcal{N}(\mu_\sigma, \sigma_\sigma^2)$, i.e.,

$$\sigma = \mu_\sigma + v\sigma_\sigma \quad (35)$$

⁶When the accuracy is higher, it means that the CRB is smaller. This convention is used throughout the paper.

where v is another Gaussian random variable with zero mean and unit standard deviation. Assume that u and σ are independent of each other. The moment generating function of ζ is given by [17]

$$\begin{aligned} \mathbb{E}_\zeta\{e^{k\zeta}\} &= \frac{1}{2\pi} \int_{-\infty}^{\infty} \int_{-\infty}^{\infty} e^{ku\sigma} e^{-(1/2\sigma_u^2)(u-\mu_u)^2} e^{-(1/2\sigma_\sigma^2)(\sigma-\mu_\sigma)^2} dud\sigma \\ &= \frac{1}{\sqrt{1-k^2\sigma_\sigma^2}} e^{(1/2(1-k^2\sigma_\sigma^2))\mu_\sigma^2 k^2} \end{aligned} \quad (36)$$

where k is a variable independent of ζ . Note that $\mathbb{E}_\zeta\{e^{k\zeta}\}$ exists when $\sigma_\sigma^2 < 1/k^2$. When $\sigma_\sigma^2 \geq 1/k^2$, the above integral will diverge. Since ε is random, we consider its statistical mean from $\bar{\varepsilon} = \mathbb{E}_\zeta\{\varepsilon\} = \mathbb{E}_\zeta\{e^{-(1/2)\nu\zeta}\}$. Substituting $k = -(1/2)\nu$ into (36), we obtain

$$\bar{\varepsilon} = \frac{1}{\sqrt{1-\frac{1}{4}\nu^2\sigma_\sigma^2}} e^{(1/2(1-(1/4)\nu^2\sigma_\sigma^2))(1/4)\nu^2\mu_\sigma^2}. \quad (37)$$

Note that we have $\varepsilon_{\text{CRB}}(\zeta) \geq \varepsilon_{\text{CRB}}(\zeta = 0)$, where the equality holds for $\sigma_\sigma = 0$ and $\mu_\sigma = 0$. The ratio $\bar{\varepsilon}$ exists and is finite when $\sigma_\sigma < (1/\nu)2 \simeq 8.6859$. When $\sigma_\sigma \geq (1/\nu)2$, the ratio becomes infinite. Actually, the condition $\sigma_\sigma \geq (1/\nu)2$ means that the shadowing is so uncertain (with too large variance) that no reliable estimate about the MS position can be provided. In a realistic scenario, it is shown in [13] that σ_σ takes the values from 1.6 to 3.0.

A. Asymptotic Cramér–Rao Bound

One way to investigate the fluctuation effects is to take the expectation of the deterministic CRB with respect to ζ . The statistical average of the deterministic CRB with respect to the random nuisance is referred to as the asymptotic CRB [18]. In this subsection, the expectation of \mathbf{B}_p in (23) with respect to ζ can be given by, at first, considering $\mathbb{E}_\zeta\{1/\tilde{\xi}\} = \mathbb{E}_\zeta\{e^{-\nu\zeta}\}$. Substituting $k = -\nu$ into (36), we obtain

$$\mathbb{E}_\zeta\{e^{-\nu\zeta}\} = \varpi \quad (38)$$

where ϖ is defined by

$$\varpi = \frac{1}{\sqrt{1-\nu^2\sigma_\sigma^2}} e^{(1/2(1-\nu^2\sigma_\sigma^2))\mu_\sigma^2\nu^2}. \quad (39)$$

The ACRB is thus given by

$$\bar{\mathbf{B}}_p = \mathbb{E}_\zeta\{\mathbf{B}_p\} = \frac{4\pi^2 f_0^2}{d_0^{-2} \text{SNR} \beta^2} \varpi (\Phi \mathbf{A}(\varrho) \Phi^T)^{-1}. \quad (40)$$

In the stochastic model, the factor ζ , which appears in the ACRB in (40) in terms of its mean and variance, primarily represents the large attenuation. The ACRB in (40) is the average of (23) over all the realizations of the random shadowing. This bound exists when $\sigma_\sigma < 1/\nu \simeq 4.343$. Note that when the shadowing disappears, the stochastic model becomes the deterministic model. This can be verified by substituting $\sigma_\sigma = 0$ and $\mu_\sigma = 0$ into the ACRB in (40), which yields the same result as the CRB in (23) for $\xi = 1$. The larger the standard deviation

σ_σ and the mean μ_σ , the more the attenuated power to each BS receiver, which leads to worse geolocation performance.

B. Simplified Bayesian Cramér–Rao Bound

Here the shadowing is considered as a random and unknown parameter with the moment generating function in (36). The performance bound in what follows is rather attractive in that the bound is easy to compute and can well approximate the sophisticated BCRB presented in the next section. Therefore, we will call this performance bound as the simplified BCRB.

From (84) in the Appendix, we have $\tilde{\mathbf{h}}_{\mathcal{T}\xi} = \mathbb{E}_\varsigma\{\tilde{\mathbf{h}}_{\mathcal{T}\xi}\} = \tilde{\mathbf{h}}_{\mathcal{T}\xi}$, $\bar{\mathbf{h}}_{\mathcal{T}\xi} = \mathbb{E}_\varsigma\{\bar{\mathbf{h}}_{\mathcal{T}\xi}\} = \bar{\mathbf{h}}_{\mathcal{T}\xi}$. Let us consider the expectation $\mathbb{E}_\xi\{\xi\} = \mathbb{E}_\varsigma\{e^{\nu\varsigma}\}$. Substituting $k = \nu$ into (36), we obtain

$$\mathbb{E}_\varsigma\{e^{\nu\varsigma}\} = \varpi. \quad (41)$$

Taking the expectation with respect to $\tilde{\xi}$ on both sides of (79) based on the elements from (84) and then using the result of (41), the expectation of the relevant FIMs with respect to ς is given by (42) shown at the bottom of the page, where $\bar{h}_{\xi\xi} = \mathbb{E}_{\tilde{\xi}}\{h_{\xi\xi}\}$ is given by

$$\bar{h}_{\xi\xi} = \kappa d_0^\gamma \text{SNR} \varpi \mathbf{1}^T \mathbf{D}^{-\gamma}(\mathbf{d}) \mathbf{1}. \quad (43)$$

Taking the block inverse of (42) (see, e.g., from (80) to (83)), we obtain the SBCRB for the model with the unknown $\tilde{\xi}$ from

$$\begin{aligned} \check{\mathbf{B}}_{\mathbf{p}} &= \frac{1}{\kappa d_0^\gamma \text{SNR} \varpi} c^2 \left(\bar{\Phi} \mathbf{D}^{-(1/2)\gamma}(\bar{\mathbf{d}}) \left(4\bar{\beta}^2 \mathbf{I} + c^2 \gamma^2 \mathbf{D}^{-1}(\bar{\mathbf{d}}) \right) \right. \\ &\quad \left. \left(\mathbf{I} - \mathbf{D}^{-(1/2)\gamma}(\bar{\mathbf{d}}) \bar{\Psi}(\bar{\varrho}) \mathbf{D}^{-(1/2)\gamma}(\bar{\mathbf{d}}) \right) \mathbf{D}^{-1}(\bar{\mathbf{d}}) \right) \\ &\quad \cdot \mathbf{D}^{-(1/2)\gamma}(\bar{\mathbf{d}}) \bar{\Phi}^T)^{-1} \\ &= \frac{4\pi^2 f_0^2}{d_0^{\gamma-2} \text{SNR} \bar{\beta}^2 \varpi} \left(\bar{\Phi} \mathbf{A}(\bar{\varrho}) \bar{\Phi}^T \right)^{-1} \end{aligned} \quad (44)$$

where $\bar{\varrho}$ is given by

$$\begin{aligned} \bar{\varrho} &= \frac{1}{1 - \nu^2 \sigma_\sigma^2} e^{(1/(1-\nu^2 \sigma_\sigma^2)) \mu_\sigma^2 \nu^2} \mathbf{1}^T \mathbf{D}^{-\gamma}(\mathbf{d}) \mathbf{1} - \mathbf{1}_M^T \\ &\quad \left(\frac{1}{4\bar{\beta}^2} c^2 \gamma^2 \mathbf{D}^{-(\gamma+2)}(\bar{\mathbf{d}}) + \mathbf{D}^{-\gamma}(\bar{\mathbf{d}}) \right) \mathbf{1}_M \\ &= (\varpi^2 - 1) \mathbf{1}^T \mathbf{D}^{-\gamma}(\mathbf{d}) \mathbf{1} + \varrho. \end{aligned} \quad (45)$$

The quantity $\bar{\varrho}$ in (45) is a (logarithmically) convex function of μ_σ on $(-\infty, \infty)$ for a fixed σ_σ and an increasing function of σ_σ

for a fixed μ_σ . It can be proved that the SBCRB is a (logarithmically) concave function of μ_σ on $(-\infty, \infty)$ for a fixed σ_σ and a decreasing function of σ_σ for a fixed μ_σ . Note that the SBCRB exists when $1 - \nu^2 \sigma_\sigma^2$ is larger than zero. As $1 - \nu^2 \sigma_\sigma^2 < 1$, this leads to the result that the quantity $1/(1 - \nu^2 \sigma_\sigma^2)$ is larger than 1. Since $\mu_\sigma^2 \nu^2$ is positive, the exponential term $e^{(1/(1-\nu^2 \sigma_\sigma^2)) \mu_\sigma^2 \nu^2}$ is larger than 1. Then, $\bar{\varrho}$ in (45) is larger than ϱ in (28). Considering the structure of (24), we can see that the difference matrix $\mathbf{A}(\bar{\varrho}) - \mathbf{A}(\varrho)$ is given by

$$\begin{aligned} \mathbf{A}(\bar{\varrho}) - \mathbf{A}(\varrho) &= \frac{1}{4\bar{\beta}^2} c^2 \gamma^2 \mathbf{D}^{-(\gamma+1)}(\bar{\mathbf{d}}) (\bar{\Psi}(\varrho) - \bar{\Psi}(\bar{\varrho})) \mathbf{D}^{-(\gamma+1)}(\bar{\mathbf{d}}) \\ &= \frac{1}{4\bar{\beta}^2} c^2 \gamma^2 \left(\frac{1}{\varrho} - \frac{1}{\bar{\varrho}} \right) \mathbf{D}^{-(\gamma+1)}(\bar{\mathbf{d}}) \mathbf{1}_{B-M} \mathbf{1}_{B-M}^T \mathbf{D}^{-(\gamma+1)}(\bar{\mathbf{d}}) \end{aligned} \quad (46)$$

which is positive definite, i.e., $\mathbf{A}(\bar{\varrho}) \succeq \mathbf{A}(\varrho)$, for $\varrho > 0$ and $\bar{\varrho} > 0$. Considering the shadowing terms ϖ in (40) and $1/\varpi$ in (44), we can see that the expectation in (38) is larger than 1, while the inverse of (41), appeared in the SBCRB at the second equality of (44), is positive but less than 1. Furthermore, when σ_σ and μ_σ are zeros, we have $\bar{\varrho}(\mu_\sigma = 0, \sigma_\sigma = 0) = \varrho(\mu_\sigma = 0, \sigma_\sigma = 0)$, which means the SBCRB is equivalent to the ACRB and both reduce to the deterministic CRB for $\xi = 1$. From these considerations, we can conclude that the SBCRB is less than or equal to the ACRB.

C. Bayesian Cramér–Rao Bound

In [8, p. 72], a bound similar to the CRB is developed when the parameter is random. In a Bayesian philosophy, the principle of an optimal estimator exploits both the received information and the *a priori* information. The BCRB and the corresponding maximum *a posteriori* estimator lie in the Bayesian method when we know the *a priori* knowledge of the model parameter. The disadvantage of the Bayesian idea is, for example, that the *a priori* information may be incorrect or we need to estimate it, which results in more complexity. Let the function $f_{\boldsymbol{\theta}}(\boldsymbol{\theta})$ be the PDF of the unknown model parameter $\boldsymbol{\theta}$. When there is no knowledge of \mathbf{p} and \mathbf{l} , the PDFs of \mathbf{p} and \mathbf{l} are uniform and then the *a priori* knowledge of the desired parameter reduces to the PDF of $\tilde{\xi}$. In general, if the *a priori* knowledge $f_{\boldsymbol{\theta}}(\boldsymbol{\theta})$ is available, the total information matrix is calculated from (see, e.g., [8, p. 84], [19, p. 930])

$$\check{\mathbf{H}}_{\boldsymbol{\theta}\boldsymbol{\theta}} = \bar{\mathbf{H}}_{\boldsymbol{\theta}\boldsymbol{\theta}} + \tilde{\mathbf{H}}_{\boldsymbol{\theta}\boldsymbol{\theta}} \quad (47)$$

$$\bar{\mathbf{H}}_{\boldsymbol{\theta}\boldsymbol{\theta}} = \mathbb{E}_\varsigma\{\mathbf{H}_{\boldsymbol{\theta}\boldsymbol{\theta}}\} = \begin{bmatrix} \frac{1}{c^2} \bar{\Phi} \tilde{\mathbf{H}}_{\mathcal{T}\mathcal{T}} \bar{\Phi}^T + \frac{1}{c^2} \bar{\Phi} \bar{\mathbf{H}}_{\mathcal{T}\mathcal{T}} \bar{\Phi}^T & \frac{1}{c^2} \bar{\Phi} \tilde{\mathbf{H}}_{\mathcal{T}\mathcal{T}} & \frac{1}{c} \bar{\Phi} \tilde{\mathbf{h}}_{\mathcal{T}\xi} + \frac{1}{c} \bar{\Phi} \bar{\mathbf{h}}_{\mathcal{T}\xi} \\ \frac{1}{c^2} \tilde{\mathbf{H}}_{\mathcal{T}\mathcal{T}} \bar{\Phi}^T & \frac{1}{c^2} \tilde{\mathbf{H}}_{\mathcal{T}\mathcal{T}} & \frac{1}{c} \tilde{\mathbf{h}}_{\mathcal{T}\xi} \\ \frac{1}{c} \tilde{\mathbf{h}}_{\mathcal{T}\xi}^T \bar{\Phi}^T + \frac{1}{c} \bar{\mathbf{h}}_{\mathcal{T}\xi}^T \bar{\Phi}^T & \frac{1}{c} \tilde{\mathbf{h}}_{\mathcal{T}\xi}^T & \frac{1}{c} \bar{\mathbf{h}}_{\mathcal{T}\xi}^T \end{bmatrix} \quad (48)$$

where the received information matrix $\bar{\mathbf{H}}_{\theta\theta} \in \mathbb{R}^{(M+3) \times (M+3)}$ and the *a priori* information matrix $\tilde{\mathbf{H}}_{\theta\theta} \in \mathbb{R}^{(M+3) \times (M+3)}$ are given by

$$\bar{\mathbf{H}}_{\theta\theta} = -\mathbb{E}_{\mathbf{r}, \boldsymbol{\theta}} \left\{ \frac{\partial^2}{\partial \boldsymbol{\theta} \partial \boldsymbol{\theta}^T} \ln(f_{\mathbf{r}|\boldsymbol{\theta}}(\mathbf{r}|\boldsymbol{\theta})) \right\} \quad (48a)$$

$$\tilde{\mathbf{H}}_{\theta\theta} = -\mathbb{E}_{\xi} \left\{ \frac{\partial^2}{\partial \boldsymbol{\theta} \partial \boldsymbol{\theta}^T} \ln(f_{\boldsymbol{\theta}}(\boldsymbol{\theta})) \right\}. \quad (48b)$$

The total FIM of the BCRB means that not only the additional information due to the *a priori* knowledge is appended to the conventional FIM, but also the usual FIM is averaged over the random parameter (otherwise the conventional FIM remains random), which is similar to the modified FIM. The Bayesian CRB is the bound that does not depend on any specific trial [19, p. 930]. Therefore, the expectation should be also taken over the realization of the model parameter $\boldsymbol{\theta}$, or more precisely $\tilde{\xi}$. An explicit statement of the additional expectation can be found in e.g., [20, eq. (10)]. In the literature, this additional information is called the Fisher information number [21]. In this model, we assume that the shadow fading $\tilde{\xi}$ is random. The *a priori* PDF is therefore given by $f_{\boldsymbol{\theta}}(\boldsymbol{\theta}) = f_{\tilde{\xi}}(\tilde{\xi})$. The *a priori* information matrix can be written as

$$\tilde{\mathbf{H}}_{\theta\theta} = \begin{bmatrix} \mathbf{0} & \mathbf{0} & \mathbf{0} \\ \mathbf{0} & \mathbf{0} & \mathbf{0} \\ \mathbf{0}^T & \mathbf{0}^T & \tilde{h}_{\xi\xi} \end{bmatrix} \quad (49)$$

where $\tilde{h}_{\xi\xi}$ is given by

$$\tilde{h}_{\xi\xi} = \frac{1}{2\nu\pi\sigma_\sigma} e^{-(1/2\sigma_\sigma^2)\mu_\sigma^2} \int_{-\infty}^{\infty} \frac{1}{\xi^2 g_\xi(\xi)} h_\xi^2(\xi) d\xi \quad (50)$$

with

$$h_\xi(\xi) = \int_0^\infty h(\xi, \omega) d\omega - \int_{-\infty}^0 h(\xi, \omega) d\omega, \quad (51a)$$

$$h(\xi, \omega) = \frac{1}{\omega} \left(\frac{1}{\nu\sigma_\sigma\omega^2} \left(\mu_\sigma - \frac{1}{\nu} \ln(\xi) \frac{1}{\omega} \right) - 1 \right) \quad (51b)$$

$$e^{-(1/2\sigma_\sigma^2)(\sigma_\sigma^2\omega^2 - (1/\nu)2\mu_\sigma \ln(\xi)1/\omega + (1/\nu^2) \ln^2(\xi)1/\omega^2)} \quad (51c)$$

and

$$g_\xi(\xi) = \int_0^\infty g(\xi, \omega) d\omega - \int_{-\infty}^0 g(\xi, \omega) d\omega \quad (52a)$$

$$g(\xi, \omega) = \frac{1}{\omega} e^{-(1/2\sigma_\sigma^2)(\sigma_\sigma^2\omega^2 - (1/\nu)2\mu_\sigma \ln(\xi)1/\omega + (1/\nu^2) \ln^2(\xi)1/\omega^2)} \quad (52b)$$

for a dummy variable ω . Taking the block inverse of (47) [see, e.g., from (80) to (83)], the BCRB is thus given by

$$\check{\mathbf{B}}_{\mathbf{p}} = c^2 \left(\bar{\boldsymbol{\Phi}} \left(\bar{\mathbf{H}}_{\mathcal{T}\mathcal{T}} - \frac{1}{\beta} \bar{\mathbf{h}}_{\mathcal{T}\xi} \bar{\mathbf{h}}_{\mathcal{T}\xi}^T \right) \bar{\boldsymbol{\Phi}}^T \right)^{-1} \\ = \frac{4\pi^2 f_0^2}{d_0^{\gamma-2} \text{SNR} \beta^2} \frac{1}{\varpi} (\bar{\boldsymbol{\Phi}} \mathbf{A}(\check{\varrho}) \bar{\boldsymbol{\Phi}}^T)^{-1} \quad (53)$$

$$\check{\varrho} = \frac{16\pi^2 f_0^2}{c^2 d_0^{\gamma-2} \text{SNR}} \frac{1}{\varpi} \tilde{h}_{\xi\xi} + \check{\varrho}. \quad (54)$$

The BCRB shown above is optimal, because all the knowledge of the model is adopted. Unfortunately, its expression is unattractive, since it involves a lot of complicate integrations.

Compared with the $\check{\varrho}$ in (45), the $\check{\varrho}$ in (54) contains an additional term due to the *a priori* knowledge of the shadowing PDF. However, if the bandwidth of the transmitted signal is large, the effects of $\check{\varrho}$ and $\check{\varrho}$ to the relevant bounds are slight.

Remark 1: Let $\varepsilon_{\text{ACRB}}$, $\varepsilon_{\text{SBCRB}}$, and $\varepsilon_{\text{BCRB}}$ be the ACRB, SBCRB, and BCRB of the estimate of the mobile position in both axes:

$$\varepsilon_{\text{ACRB}} = \sqrt{\text{tr}(\bar{\mathbf{B}}_{\mathbf{p}})}, \quad \varepsilon_{\text{SBCRB}} = \sqrt{\text{tr}(\check{\mathbf{B}}_{\mathbf{p}})}, \quad \varepsilon_{\text{BCRB}} = \sqrt{\text{tr}(\check{\mathbf{B}}_{\mathbf{p}})}. \quad (55)$$

Since $\tilde{h}_{\xi\xi} = \mathbb{E}_{\xi} \left\{ ((\partial/\partial\xi) \ln(f_\xi(\xi)))^2 \right\} \geq 0$, we have

$$\check{\varrho} \geq \check{\varrho} \Rightarrow \frac{1}{\check{\beta}} \leq \frac{1}{\beta} \\ \Rightarrow \bar{\boldsymbol{\Phi}} \left(\bar{\mathbf{H}}_{\mathcal{T}\mathcal{T}} - \frac{1}{\beta} \bar{\mathbf{h}}_{\mathcal{T}\xi} \bar{\mathbf{h}}_{\mathcal{T}\xi}^T \right) \bar{\boldsymbol{\Phi}}^T \succeq \bar{\boldsymbol{\Phi}} \left(\bar{\mathbf{H}}_{\mathcal{T}\mathcal{T}} - \frac{1}{\check{\beta}} \bar{\mathbf{h}}_{\mathcal{T}\xi} \bar{\mathbf{h}}_{\mathcal{T}\xi}^T \right) \bar{\boldsymbol{\Phi}}^T \\ \Rightarrow \check{\mathbf{B}}_{\mathbf{p}}^{-1} \succeq \bar{\mathbf{B}}_{\mathbf{p}}^{-1} \\ \Rightarrow \check{\mathbf{B}}_{\mathbf{p}} \preceq \bar{\mathbf{B}}_{\mathbf{p}} \\ \Rightarrow \varepsilon_{\text{BCRB}} \leq \varepsilon_{\text{SBCRB}}. \quad (56)$$

Using the condition $\lim_{\text{SNR} \rightarrow \infty} \check{\varrho} = \check{\varrho}$, we obtain

$$\lim_{\text{SNR} \rightarrow \infty} \varepsilon_{\text{BCRB}} = \varepsilon_{\text{SBCRB}}. \quad (57)$$

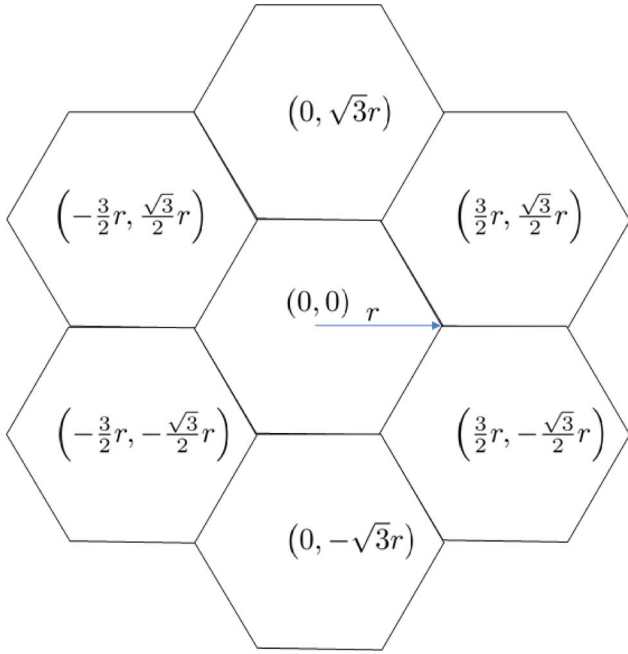
We can verify that the BCRB is upper bounded by the SBCRB and the bound equality holds for a high SNR.

Remark 2: The equality also holds when ξ is known. This is because the matrix $\boldsymbol{\Psi}(\check{\varrho})$ becomes zero and thus the BCRB is equal to the SBCRB. The result is reasonable, because the information of $f_\xi(\xi)$ is useless if ξ is known. However, if ξ is unknown, we have

$$\varepsilon_{\text{BCRB}} \leq \varepsilon_{\text{SBCRB}} \leq \varepsilon_{\text{ACRB}}. \quad (58)$$

The information of $f_\xi(\xi)$ is still useful even for a high SNR, since $\lim_{\text{SNR} \rightarrow \infty} \varepsilon_{\text{BCRB}} = \varepsilon_{\text{SBCRB}} \leq \varepsilon_{\text{ACRB}}$. For $\mu_\sigma = 0$ and $\sigma_\sigma = 0$, the asymptotic large SNR makes the BCRB trivial, since

$$\lim_{\text{SNR} \rightarrow \infty} \varepsilon_{\text{BCRB}}(\mu_\sigma = 0, \sigma_\sigma = 0) = \varepsilon_{\text{SBCRB}}(\mu_\sigma = 0, \sigma_\sigma = 0) \\ = \varepsilon_{\text{ACRB}}(\mu_\sigma = 0, \sigma_\sigma = 0).$$

Fig. 1. Cellular system with cell radius r .

V. NUMERICAL EXAMPLES

Consider a certain configuration of a cellular system. In seven hexagonal cells, there is a MS locating in the central cell, i.e., $\mathbf{p} = [0 \ 0]^T$. The BSs are located at the center of each cell according to Fig. 1 with the position matrix

$$\mathbf{P} = \begin{bmatrix} \frac{3}{2} & 0 & -\frac{3}{2} & -\frac{3}{2} & 0 & \frac{3}{2} \\ \frac{\sqrt{3}}{2} & \sqrt{3} & \frac{\sqrt{3}}{2} & -\frac{\sqrt{3}}{2} & -\sqrt{3} & -\frac{\sqrt{3}}{2} \end{bmatrix}^T r \quad (59)$$

where r is the cell radius. The associated angles of the BSs become

$$\phi = \frac{1}{6} [1 \ 3 \ 5 \ 7 \ 9 \ 11]^T \pi. \quad (60)$$

We assume that the first M BSs receive the NLoS signals. Then, the distances between the LoS BSs and the MS are given by $d_b = \sqrt{3}r$; $b \in \{M+1, M+2, \dots, 6\}$. The system is assumed to operate under the central frequency of 1.9 GHz [13] and effective bandwidth $\bar{\beta} = (1/\sqrt{3})10\pi$ MHz [22]. In this scenario, the cell radius (r) is 2000 m and the close-in distance (d_0) is 100 m. For the NLoS, the additional path distance is assumed to be $l = 10$ m as the default value, whereas the length of up to several kilometers has no significant impact, except for a low bandwidth. We determine the path exponent from $\gamma = a + bh_b + (1/h_b)c$, where a , b , and c are given from [13] with the antenna height $h_b = 45$ m.

In what follows, we consider three terrain categories [13]: A (hilly/moderate-to-heavy tree density with $\mu_\sigma = 10.6$ and $\sigma_\sigma = 2.3$), B (hilly light tree density or flat/moderate-to-heavy tree density with $\mu_\sigma = 9.6$ and $\sigma_\sigma = 3.0$) and C (flat/light tree density with $\mu_\sigma = 8.2$ and $\sigma_\sigma = 1.6$). In Fig. 2, the error variance ε_{CRB} of the deterministic CRB in (23) and ϱ in (28) are shown as functions of the additional NLoS path length for $M = 1$, and $\bar{\beta} = 18.138$ kHz and $\bar{\beta} = 18.138$ MHz. In this

situation, the transmitted SNR and the shadow fading are assumed to be SNR = 100 dB and $\xi = 40$ dB. We consider the environment A, which provides the same trend as that given by the environments B and C. It can be seen that when the signal bandwidth is in the order of kHz, the CRB slightly changes with l for $l \in [0.0, 2.0]$ km and $l \in [2.5, 4]$ km. For a small interval of $l \in [2.0, 2.5]$ km, the CRB changes dramatically. It can be explained as follows. In (23), the CRB for the case of the deterministic but unknown channel fading depends on the NLoS. This is because in the calculation of Ψ in (27), the second term of ϱ relies on the NLoS mobile positions in $\hat{\mathbf{d}}$. For the effective bandwidth of the signal on the order of kilohertz, the second term $(1/4\bar{\beta}^2)c^2\gamma^2 \sum_{b=1}^M 1/(\sqrt{\tilde{x}_b^2 + \tilde{y}_b^2} + l_b)^{\gamma+2}$ in (28) is dominant and ϱ can be zero. When ϱ is close to zero for $l \in [2.00, 2.25]$ in the upper left plot in Fig. 2, there exists a turning point in the CRB. When ϱ approaches zero from minus side, i.e., $\lim_{l \rightarrow 2.25^-} \varrho \cong 0^-$, Ψ tends to be negatively infinite, i.e., $\lim_{\varrho \rightarrow 0^-} [\Psi]_{[n, \hat{n}]} = -\infty$; $n, \hat{n} \in \{1, 2, \dots, B-M\}$. The bound in this region drops to zero, since $\lim_{\varrho \rightarrow 0^-} \mathbf{A}^{-1} = \mathbf{O}$. On

the other hand, when ϱ gradually goes beyond zero to the positive side for $l \in [2.25, 2.50]$ km, i.e., $\lim_{l \rightarrow 2.25^+} \varrho \cong 0^+$, Ψ has the elements of positive and large values, i.e., $\lim_{\varrho \rightarrow 0^+} [\Psi]_{[n, \hat{n}]} = \infty$; $n, \hat{n} \in \{1, 2, \dots, B-M\}$. This leads to that the CRB changes dramatically in the positive side of ϱ . For a positive ϱ , the lower the value of ϱ , the larger the value of the elements in Ψ , and hence the lower the CRB \mathbf{B}_p . The turning point can be observed in Fig. 2 for the case of $\bar{\beta} = 18.138$ kHz from $l = 2.5$ km to $l = 2.25$ km. It comes from the zero value of the Schur complement in (81), which means that the estimation of the shadowing ξ and the subsequent parameters, such as the excess path length l_b and the mobile position \mathbf{p} , is infeasible. Therefore, in this model, there exist some values of l_b and $\bar{\beta}$ such that we cannot estimate the mobile position. However, this situation happens rarely in a modern wireless system, because the signal typically possesses a large bandwidth. When the effective bandwidth of the signal $\bar{\beta}$ is large, e.g., in the order of MHz, the role of the NLoS in (28) can be neglected. The behavior of the almost constant CRB is illustrated in the right plots of Fig. 2. When the signal bandwidth is in the order of MHz, the CRB in the lower right plot of Fig. 2 decreases monotonously with l and finally converges to a constant as l approaches the infinity. In both signal bandwidths, the wireless NLoS geolocation provides a fixed error performance for the large excess NLoS path length. From the physical point of view, this asymptotic behavior comes from the fact that the system invokes only the LoS signals, while the NLoS contribution disappears when l becomes very large.

In Fig. 3, the excess path length, the transmitted SNR and the shadow fading are chosen as $l = 3200$ m, SNR = 100 dB and $\xi = 40$ dB, respectively. The BSs are assumed to be located on a circle line each with an identical sector and the radial distance between the BSs and the MS of $(1/\sqrt{3})2000$ m. In this NLoS geolocation problem, it can be shown that the ML estimate of \mathbf{p} can be calculated when $B - M \geq 2$. Therefore, we keep $B - M = 2$. It can be seen that for $B = 3$ and $\bar{\beta} = 18.138$ kHz,

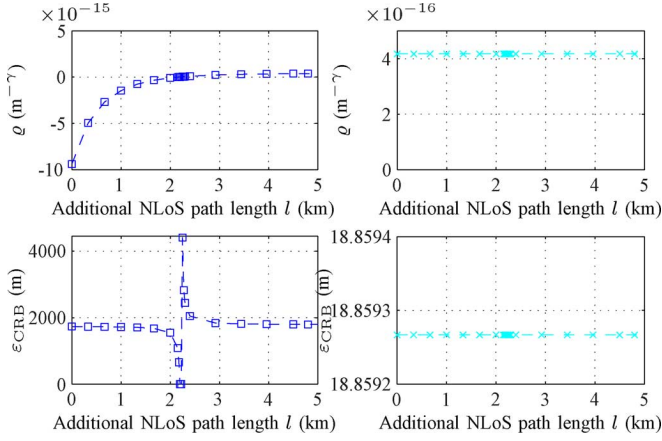


Fig. 2. CRB in (23) and ϱ in (28) as functions of the additional NLoS path length l . The terrain A and $M = 1$ are considered. Left plots invoke $\bar{\beta} = 18.138$ kHz. Right plots adopt $\bar{\beta} = 18.138$ MHz.

ϱ is larger than zero. From $B = 3$ to $B = 4$, the bound increases greatly. However, for $\bar{\beta} = 18.138$ MHz, the bound decreases from $B = 3$ to $B = 4$. As investigated the whole range of the BS number, we can see that the bound increases with the number of BSs, except for the case $B = 3$ where the bound is sensitive to the additional NLoS path length l and the effective bandwidth of the signal, due to few BSs receiving the LoS. It can be inferred from Fig. 3 that the BS with the NLoS measurement plays a role of increasing the uncertainty for the position estimation instead of increasing the accuracy. Thus, adding the NLoS measurement data to the observation set is detrimental, instead of instrumental, to the localization problem. The physical meaning of this phenomenon is that the performance of the mobile position estimation degrades with more uncertain observations. In Fig. 4, the cellular geometry is adopted and the deterministic CRB calculated by (23) is shown as a function of the shadow fading ξ . We can see that for a fixed number of the BSs receiving the NLoS signals, the shadow fading affects the accuracy of the mobile position estimate. The shadowing reduces the CRB in the same manner as the SNR. Furthermore, when the number of the NLoS BSs is increased from one to three, the CRB of the mobile position estimate is increased accordingly. This is because the more the number of the NLoS BSs, the more the inaccurate received data.

In Fig. 5, the ACRB and the SBCRB are shown as a function of σ_σ . For $0 < \sigma_\sigma < 1/\nu \approx 4.3429$, the ACRB considerably increases and the SBCRB gradually decreases with σ_σ . It can be seen that the higher the μ_σ , the higher the ACRB and the lower the SBCRB. The reason that the SBCRB is lower than the ACRB is based on the Jensen's inequality of $\left(E_{\xi} \{ \mathbf{H} \boldsymbol{\theta} \boldsymbol{\theta}^T (\xi) \} \right)^{-1} \leq E_{\xi} \{ \mathbf{H} \boldsymbol{\theta} \boldsymbol{\theta}^T (\xi) \}^{-1}$. In Fig. 6, the positioning accuracy is computed for 1) A ($\mu_\sigma = 10.6, \sigma_\sigma = 2.3$), 2) B ($\mu_\sigma = 9.6, \sigma_\sigma = 3.0$), and 3) C ($\mu_\sigma = 8.2, \sigma_\sigma = 1.6$). The asymptotic, modified and Bayesian CRBs are calculated from (40), (44), and (53), respectively. We can see that the SBCRB and the BCRB almost coincide with each other, while the ACRB is higher than the SBCRB and the BCRB. In the wireless geolocation, when the shadowing effect is explored in the channel model, the transmitter needs to transmit a very large SNR in order to obtain a

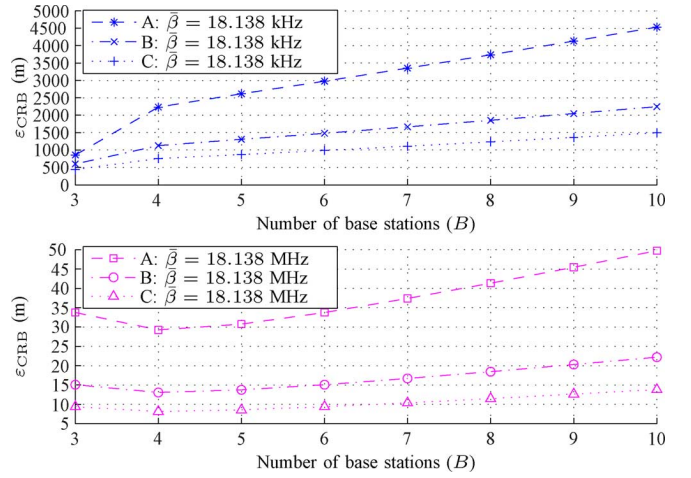


Fig. 3. CRB in (23) as a function of the number of BSs B .

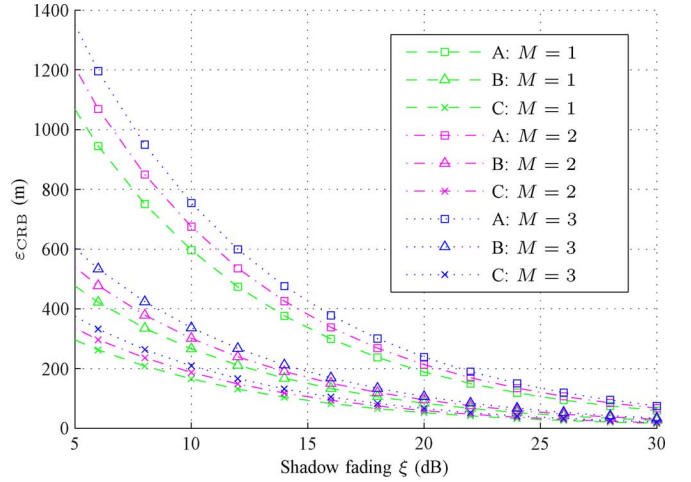


Fig. 4. CRB in (23) as a function of the shadow fading ξ .

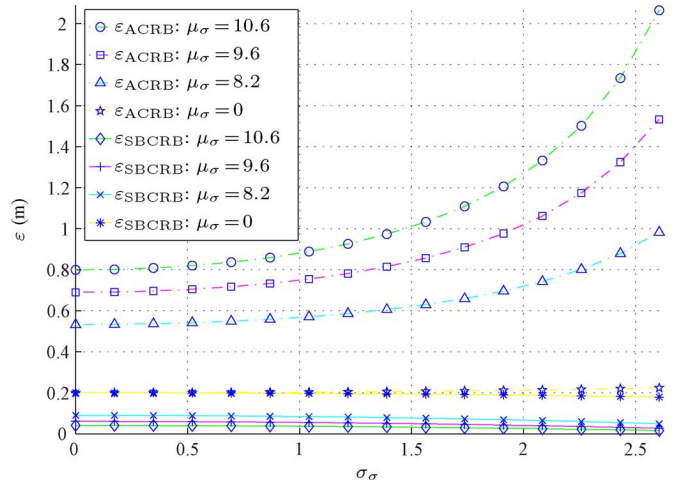


Fig. 5. ACRB in (40) and the SBCRB in (44) as a function of σ_σ . The corresponding parameters are as follows: $\bar{\beta} = (1/\sqrt{3})10\pi$ MHz, SNR = 100 dB, $B = 6, M = 1, r = 2000$ m, $l = 10$ m, $f_0 = 1.9$ GHz, and $d_0 = 100$ m.

considerable accuracy. This high energy transmission therefore makes the SBCRB and the BCRB almost coincided with each

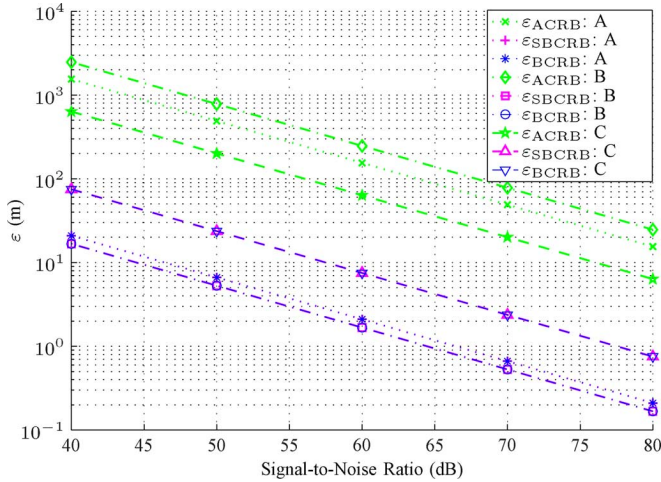


Fig. 6. Positioning accuracy as a function of SNR. The corresponding parameters are as follows: $\beta = (1/\sqrt{3})10\pi$ MHz, $B = 6$, $M = 1$, $r = 2000$ m, $l = 10$ m, $f_0 = 1.9$ GHz and $d_0 = 100$ m.

other. Note that the BCRB involves with the numerical integrations. In the above figure, the SBCRB, which is much computationally simpler, can well approximate the BCRB. Based on this approximation, it can be inferred that if the *a priori* knowledge of the shadow fading is available, the BCRB is equivalent to the SBCRB in Fig. 5. Then, we can see that the performance bound derived from the available *a priori* knowledge gradually decreases with the increase of μ_σ and σ_σ . This performance improvement can be physically viewed from the use of the additional knowledge available in the system.

VI. CONCLUSION

The inherent accuracy limitation of the wireless geolocation in the mixed LoS/NLoS environments without the NLoS mitigation is investigated in the presence of the shadowing. We derive the CRB for the deterministic shadowing, the ACRB and the SBCRB for the random shadowing, and the BCRB for the random shadowing with the *a priori* knowledge of the shadowing PDF. It is shown that the CRB and its variants depend on the additional length of the NLoS path. In deterministic case, the numerical examples show that for the effective bandwidth in the order of kHz, the CRB almost does not change with the additional length of the NLoS path except for a small interval of the length, in which the CRB changes dramatically. For the effective bandwidth in the order of MHz, the CRB decreases monotonously with the additional length of the NLoS path and finally converges to a constant as the additional length of the NLoS path approaches the infinity. It is shown that the BS with the NLoS measurement plays a role of increasing the uncertainty for the position estimation instead of increasing the accuracy. The shadowing parameter ξ increases the positioning accuracy in the same way as the SNR does. In the random shadowing case, a multiplicative model of two Gaussian random variables is represented for the shadowing exponent. However, the BCRB involves with the numerical integrations. The numerical examples illustrate that the SBCRB, which is much computationally

simpler, can well approximate the BCRB. It is also indicated that when the mean μ_σ and the standard deviation σ_σ are larger, the accuracy of the mobile position estimation considerably decreases in the case of no *a priori* knowledge of the shadow fading and gradually increases when the *a priori* knowledge is available. For future works, the performance bounds shown above can be further analyzed in the multipath environment, e.g., in [23].

APPENDIX

DERIVATION OF DETERMINISTIC CRB

For a short notation, let us introduce $\vartheta \in \mathbb{R}^{(B+1) \times 1}$ as

$$\vartheta = [\tau^T \quad \xi^T]^T. \quad (61)$$

Using the chain rule, the FIM can be written as

$$\mathbf{H}_{\vartheta\vartheta} = \nabla_{\vartheta\vartheta} \mathbf{H}_{\mathbf{r}\vartheta} \nabla_{\vartheta\vartheta}^T \quad (62)$$

where $\nabla_{\vartheta\vartheta} \in \mathbb{R}^{(M+3) \times (2B+1)}$ and $\mathbf{H}_{\mathbf{r}\vartheta} \in \mathbb{R}^{(2B+1) \times (2B+1)}$ are defined by

$$\nabla_{\vartheta\vartheta} = \frac{\partial}{\partial \vartheta} \vartheta^T \quad (63a)$$

$$\mathbf{H}_{\mathbf{r}\vartheta} = -\mathbb{E}_{\mathbf{r}} \left\{ \frac{\partial^2}{\partial \vartheta \partial \vartheta^T} \ln \left(f_{\mathbf{r}|\vartheta}(\mathbf{r}|\vartheta) \right) \right\}. \quad (63b)$$

Let us first consider

$$\nabla_{\vartheta\vartheta} = \begin{bmatrix} \nabla_{\mathbf{p}\tau} & \mathbf{0} \\ \nabla_{\mathbf{l}\tau} & \mathbf{0} \\ \mathbf{0}^T & 1 \end{bmatrix} \quad (64)$$

where $\nabla_{\mathbf{p}\tau} \in \mathbb{R}^{2 \times B}$ and $\nabla_{\mathbf{l}\tau} \in \mathbb{R}^{M \times B}$ are defined by

$$\nabla_{\mathbf{p}\tau} = \frac{\partial}{\partial \mathbf{p}} \tau^T \quad (65a)$$

$$\nabla_{\mathbf{l}\tau} = \frac{\partial}{\partial \mathbf{l}} \tau^T. \quad (65b)$$

Consider

$$\mathbf{H}_{\vartheta\vartheta} = \begin{bmatrix} \mathbf{H}_{\tau\tau} & \mathbf{h}_{\tau\xi} \\ \mathbf{h}_{\tau\xi}^T & h_{\xi\xi} \end{bmatrix} \quad (66)$$

where $\mathbf{H}_{\tau\tau} \in \mathbb{R}^{B \times B}$, $\mathbf{h}_{\tau\xi} \in \mathbb{R}^{B \times 1}$, and $h_{\xi\xi} \in \mathbb{R}^{1 \times 1}$ are

$$\mathbf{H}_{\tau\tau} = -\mathbb{E}_{\mathbf{r}} \left\{ \frac{\partial^2}{\partial \tau \partial \tau^T} \ln \left(f_{\mathbf{r}|\tau}(\mathbf{r}|\tau) \right) \right\} \quad (67a)$$

$$\mathbf{h}_{\tau\xi} = -\mathbb{E}_{\mathbf{r}} \left\{ \frac{\partial^2}{\partial \tau \partial \xi} \ln \left(f_{\mathbf{r}|\tau}(\mathbf{r}|\tau) \right) \right\} \quad (67b)$$

$$h_{\xi\xi} = -\mathbb{E}_{\mathbf{r}} \left\{ \frac{\partial^2}{\partial \xi \partial \xi} \ln \left(f_{\mathbf{r}|\tau}(\mathbf{r}|\tau) \right) \right\}. \quad (67c)$$

Consider

$$\nabla_{\mathbf{p}\tau} = \frac{1}{c} [\tilde{\Phi} \quad \bar{\Phi}] \quad (68)$$

where $\tilde{\Phi} \in \mathbb{R}^{2 \times M}$ is given by

$$\tilde{\Phi} = \begin{bmatrix} \cos(\phi_1) & \cos(\phi_2) & \cdots & \cos(\phi_M) \\ \sin(\phi_1) & \sin(\phi_2) & \cdots & \sin(\phi_M) \end{bmatrix}. \quad (69)$$

The derivative $(\partial/\partial\xi)\alpha_b$ is given by

$$\frac{\partial}{\partial\xi}\alpha_b = \frac{1}{2\xi}\sqrt{\kappa} \left(\frac{d_0}{\sqrt{\tilde{x}_b^2 + \tilde{y}_b^2 + l_b}} \right)^{(1/2)\gamma} \sqrt{\xi} = \frac{1}{2\xi}\alpha_b. \quad (70)$$

According to (70), we have

$$\frac{\partial}{\partial\xi}\alpha = \frac{1}{2\xi}\alpha. \quad (71) \quad \text{and}$$

Let us introduce $\alpha^2 = \alpha \odot \alpha$. Since the signal exists from $t = 0$ to $t = T_s$, the upper limit of the integration, $t = T_o$, can be replaced with $t = T_s$. In more details, the Fisher information in (67) can be written as (72), shown at the bottom of the page. Similarly, we have

$$\mathbf{h}_{\mathcal{T}\xi} = -\mathbb{E}_{\mathbf{r}} \left\{ \frac{\partial}{\partial\tau} \left(\frac{\partial}{\partial\xi} \ln(f_{\mathbf{r}|\theta}(\mathbf{r}|\theta)) \right)^{\mathbf{T}} \right\}$$

$$\begin{aligned} &= \frac{1}{N_0} 4 \int_0^{T_s} \left(\frac{\partial}{\partial\tau} \tilde{\mathbf{s}}^{\mathbf{H}}(t, \boldsymbol{\vartheta}) \right) \left(\frac{\partial}{\partial\xi} \tilde{\mathbf{s}}(t, \boldsymbol{\vartheta}) \right) dt \\ &= \frac{1}{N_0} 4 \int_0^{T_s} \mathbf{D} \left(-\frac{1}{2} \gamma \frac{1}{\tau} \odot \alpha \odot \mathbf{s}^*(t, \tau) \right) \left(\left(\frac{1}{2\xi} \alpha \right) \odot \mathbf{s}(t, \tau) \right) dt \\ &= \frac{1}{N_0} 4 E_s \left(-\frac{1}{4\xi} \gamma \mathbf{D}(\alpha) \mathbf{D}^{-1}(\tau) \alpha \right) \\ &= \text{SNR} \left(-\frac{1}{\xi} \gamma \mathbf{D}^2(\alpha) \mathbf{D}^{-1}(\tau) \mathbf{1} \right) \end{aligned} \quad (73)$$

$$\begin{aligned} h_{\xi\xi} &= -\mathbb{E}_{\mathbf{r}} \left\{ \frac{\partial}{\partial\xi} \frac{\partial}{\partial\xi} \ln(f_{\mathbf{r}|\theta}(\mathbf{r}|\theta)) \right\} \\ &= \frac{1}{N_0} 4 \int_0^{T_s} \left(\frac{\partial}{\partial\xi} \tilde{\mathbf{s}}^{\mathbf{H}}(t, \boldsymbol{\vartheta}) \right) \left(\frac{\partial}{\partial\xi} \tilde{\mathbf{s}}(t, \boldsymbol{\vartheta}) \right) dt \\ &= \frac{1}{N_0} 4 \int_0^{T_s} \left(\frac{\partial}{\partial\xi} \alpha^{\mathbf{T}} \right) \mathbf{D}(\mathbf{s}^*(t, \tau)) \mathbf{D}(\mathbf{s}(t, \tau)) \left(\frac{\partial}{\partial\xi} \alpha \right) dt \\ &= 4 \text{SNR} \left(\frac{1}{2\xi} \alpha \right)^{\mathbf{T}} \left(\frac{1}{2\xi} \alpha \right) = \frac{1}{\xi^2} \text{SNR} \alpha^{\mathbf{T}} \alpha. \end{aligned} \quad (74)$$

$$\begin{aligned} \mathbf{H}_{\mathcal{T}\tau} &= -\mathbb{E}_{\mathbf{r}} \left\{ \frac{\partial}{\partial\tau} \left(\frac{\partial}{\partial\tau} \ln(f_{\mathbf{r}|\theta}(\mathbf{r}|\theta)) \right)^{\mathbf{T}} \right\} \\ &= \frac{1}{N_0} 2 \mathbb{E}_{\mathbf{r}} \left\{ \frac{\partial}{\partial\tau} \left(\int_0^{T_s} \frac{\partial}{\partial\tau} \|\mathbf{r}(t) - \tilde{\mathbf{s}}(t, \boldsymbol{\vartheta})\|_{\mathbb{E}}^2 dt \right)^{\mathbf{T}} \right\} \\ &= \frac{1}{N_0} 2 \mathbb{E}_{\mathbf{r}} \left\{ \frac{\partial}{\partial\tau} \int_0^{T_s} \left(\left(\frac{\partial}{\partial\tau} \tilde{\mathbf{s}}^{\mathbf{H}}(t, \boldsymbol{\vartheta}) \right) \frac{\partial}{\partial \tilde{\mathbf{s}}^*(t, \tau)} \|\mathbf{r}(t) - \tilde{\mathbf{s}}(t, \boldsymbol{\vartheta})\|_{\mathbb{E}}^2 \right)^{\mathbf{H}} dt \right\} \\ &= -\frac{1}{N_0} 4 \mathbb{E}_{\mathbf{r}} \left\{ \frac{\partial}{\partial\tau} \int_0^{T_s} (\mathbf{r}(t) - \tilde{\mathbf{s}}(t, \boldsymbol{\vartheta}))^{\mathbf{H}} \left[\frac{\partial}{\partial\tau_1} \tilde{\mathbf{s}}(t, \boldsymbol{\vartheta}) \quad \cdots \quad \frac{\partial}{\partial\tau_B} \tilde{\mathbf{s}}(t, \boldsymbol{\vartheta}) \right] dt \right\} \\ &= -\frac{1}{N_0} 4 \int_0^{T_s} - \left[\left(\frac{\partial}{\partial\tau} \tilde{\mathbf{s}}^{\mathbf{H}}(t, \boldsymbol{\vartheta}) \right) \frac{\partial}{\partial\tau_1} \tilde{\mathbf{s}}(t, \boldsymbol{\vartheta}) \cdots \left(\frac{\partial}{\partial\tau} \tilde{\mathbf{s}}^{\mathbf{H}}(t, \boldsymbol{\vartheta}) \right) \frac{\partial}{\partial\tau_B} \tilde{\mathbf{s}}(t, \boldsymbol{\vartheta}) \right] \\ &\quad + \left[\left(\frac{\partial}{\partial\tau} \frac{\partial}{\partial\tau_1} \tilde{\mathbf{s}}^{\mathbf{H}}(t, \boldsymbol{\vartheta}) \right) (\mathbb{E}_{\mathbf{r}(t)}\{\mathbf{r}(t)\} - \tilde{\mathbf{s}}(t, \boldsymbol{\vartheta})) \cdots \left(\frac{\partial}{\partial\tau} \frac{\partial}{\partial\tau_B} \tilde{\mathbf{s}}^{\mathbf{H}}(t, \boldsymbol{\vartheta}) \right) (\mathbb{E}_{\mathbf{r}(t)}\{\mathbf{r}(t)\} - \tilde{\mathbf{s}}(t, \boldsymbol{\vartheta})) \right] dt \\ &= \frac{1}{N_0} 4 \int_0^{T_s} \left(\frac{\partial}{\partial\tau} \tilde{\mathbf{s}}^{\mathbf{H}}(t, \boldsymbol{\vartheta}) \right) \left(\frac{\partial}{\partial\tau} \tilde{\mathbf{s}}^{\mathbf{H}}(t, \boldsymbol{\vartheta}) \right)^{\mathbf{H}} dt \\ &= \frac{1}{N_0} 4 \int_0^{T_s} \mathbf{D} \left(\left(\frac{\partial}{\partial\tau} \odot \alpha \right) \odot \mathbf{s}^*(t, \tau) + \alpha \odot \left(\frac{\partial}{\partial\tau} \odot \mathbf{s}^*(t, \tau) \right) \right) \mathbf{D}^{\mathbf{H}}(\cdot) dt \\ &= \frac{1}{N_0} 4 \int_0^{T_s} \mathbf{D} \left(\alpha^2 \odot \left| \frac{\partial}{\partial\tau} \odot \mathbf{s}(t, \tau) \right|^2 - \frac{1}{2} \frac{1}{\tau} \gamma \odot \alpha^2 \odot \left(\frac{\partial}{\partial\tau} \odot \mathbf{s}^*(t, \tau) \right) \odot \mathbf{s}(t, \tau) \right. \\ &\quad \left. - \frac{1}{2} \frac{1}{\tau} \gamma \odot \alpha^2 \odot \mathbf{s}^*(t, \tau) \odot \left(\frac{\partial}{\partial\tau} \odot \mathbf{s}(t, \tau) \right) + \frac{1}{4} \frac{1}{\tau^2} \gamma^2 \odot \alpha^2 \odot |\mathbf{s}(t, \tau)|^2 \right) dt \\ &= \frac{1}{N_0} 4 \left(\bar{\beta}^2 E_s \mathbf{D}^2(\alpha) + \frac{1}{4} \gamma^2 E_s \mathbf{D}^2(\alpha) \mathbf{D}^{-2}(\tau) \right) \\ &= \text{SNR} (4\bar{\beta}^2 \mathbf{D}^2(\alpha) + \gamma^2 \mathbf{D}^2(\alpha) \mathbf{D}^{-2}(\tau)). \end{aligned} \quad (72)$$

$$\mathbf{H}_{\theta\theta} = \begin{bmatrix} \nabla_{\mathbf{p}^T} & \mathbf{0} \\ \nabla_{\mathbf{r}^T} & \mathbf{0} \\ \mathbf{0}^T & 1 \end{bmatrix} \begin{bmatrix} \mathbf{H}_{\mathcal{T}\mathcal{T}} & \mathbf{h}_{\mathcal{T}\xi} \\ \mathbf{h}_{\mathcal{T}\xi}^T & h_{\xi\xi} \end{bmatrix} \begin{bmatrix} \nabla_{\mathbf{p}^T} & \nabla_{\mathbf{r}^T} & \mathbf{0}^T \\ \mathbf{0}^T & \mathbf{0}^T & 1 \end{bmatrix} = \begin{bmatrix} \frac{1}{c^2} \tilde{\Phi} \tilde{\mathbf{H}}_{\mathcal{T}\mathcal{T}} \tilde{\Phi}^T + \frac{1}{c^2} \tilde{\Phi} \tilde{\mathbf{H}}_{\mathcal{T}\mathcal{T}} \tilde{\Phi}^T & \frac{1}{c^2} \tilde{\Phi} \tilde{\mathbf{H}}_{\mathcal{T}\mathcal{T}} & \frac{1}{c} \tilde{\Phi} \tilde{\mathbf{h}}_{\mathcal{T}\xi} + \frac{1}{c} \tilde{\Phi} \tilde{\mathbf{h}}_{\mathcal{T}\xi} \\ \frac{1}{c^2} \tilde{\mathbf{H}}_{\mathcal{T}\mathcal{T}} \tilde{\Phi}^T & \frac{1}{c^2} \tilde{\mathbf{H}}_{\mathcal{T}\mathcal{T}} & \frac{1}{c} \tilde{\mathbf{h}}_{\mathcal{T}\xi} \\ \frac{1}{c} \tilde{\mathbf{h}}_{\mathcal{T}\xi}^T \tilde{\Phi}^T + \frac{1}{c} \tilde{\mathbf{h}}_{\mathcal{T}\xi}^T \tilde{\Phi}^T & \frac{1}{c} \tilde{\mathbf{h}}_{\mathcal{T}\xi}^T & h_{\xi\xi} \end{bmatrix} \quad (79)$$

For the NLoS and the LoS portions, the diagonal matrix $\mathbf{H}_{\mathcal{T}\mathcal{T}}$ can be partitioned as

$$\mathbf{H}_{\mathcal{T}\mathcal{T}} = \begin{bmatrix} \tilde{\mathbf{H}}_{\mathcal{T}\mathcal{T}} & \mathbf{O} \\ \mathbf{O} & \tilde{\mathbf{H}}_{\mathcal{T}\mathcal{T}}, \end{bmatrix} \quad (75)$$

where $\tilde{\mathbf{H}}_{\mathcal{T}\mathcal{T}} \in \mathbb{R}^{M \times M}$ and $\tilde{\mathbf{H}}_{\mathcal{T}\mathcal{T}} \in \mathbb{R}^{(B-M) \times (B-M)}$ are given by

$$\tilde{\mathbf{H}}_{\mathcal{T}\mathcal{T}} = \text{SNR} (4\bar{\beta}^2 \mathbf{D}^2(\tilde{\boldsymbol{\alpha}}) + \gamma^2 \mathbf{D}^2(\tilde{\boldsymbol{\alpha}}) \mathbf{D}^{-2}(\tilde{\boldsymbol{\tau}})) \quad (76a)$$

$$\tilde{\mathbf{H}}_{\mathcal{T}\mathcal{T}} = \text{SNR} (4\bar{\beta}^2 \mathbf{D}^2(\bar{\boldsymbol{\alpha}}) + \gamma^2 \mathbf{D}^2(\bar{\boldsymbol{\alpha}}) \mathbf{D}^{-2}(\bar{\boldsymbol{\tau}})) \quad (76b)$$

with $\tilde{\boldsymbol{\alpha}} \in \mathbb{R}^{M \times 1}$, $\bar{\boldsymbol{\alpha}} \in \mathbb{R}^{(B-M) \times 1}$, $\tilde{\boldsymbol{\tau}} \in \mathbb{R}^{M \times 1}$ and $\bar{\boldsymbol{\tau}} \in \mathbb{R}^{(B-M) \times 1}$ given by

$$\boldsymbol{\alpha} = [\tilde{\boldsymbol{\alpha}}^T \quad \bar{\boldsymbol{\alpha}}^T]^T \quad (77a)$$

$$\boldsymbol{\tau} = [\tilde{\boldsymbol{\tau}}^T \quad \bar{\boldsymbol{\tau}}^T]^T. \quad (77b)$$

Let us partition $\mathbf{h}_{\mathcal{T}\xi}$ into

$$\mathbf{h}_{\mathcal{T}\xi} = \begin{bmatrix} \tilde{\mathbf{h}}_{\mathcal{T}\xi} \\ \bar{\mathbf{h}}_{\mathcal{T}\xi} \end{bmatrix} = -\frac{1}{\xi} \text{SNR} \gamma \begin{bmatrix} \mathbf{D}^2(\tilde{\boldsymbol{\alpha}}) \mathbf{D}^{-1}(\tilde{\boldsymbol{\tau}}) \mathbf{1}_M \\ \mathbf{D}^2(\bar{\boldsymbol{\alpha}}) \mathbf{D}^{-1}(\bar{\boldsymbol{\tau}}) \mathbf{1}_{B-M} \end{bmatrix}. \quad (78)$$

Substituting (64) and (66) into (62), we obtain (79), shown at the top of the page. Using the inverse of a partitioned matrix (see, e.g., [24, p. 123]), the CRB of the mobile position \mathbf{p} can be calculated from

$$\mathbf{B}_{\mathbf{p}}^{-1} = \frac{1}{c^2} \left(\tilde{\Phi} \tilde{\mathbf{H}}_{\mathcal{T}\mathcal{T}} \tilde{\Phi}^T + \tilde{\Phi} \tilde{\mathbf{H}}_{\mathcal{T}\mathcal{T}} \tilde{\Phi}^T \right) - \left[\frac{1}{c^2} \tilde{\Phi} \tilde{\mathbf{H}}_{\mathcal{T}\mathcal{T}} \quad \frac{1}{c} (\tilde{\Phi} \tilde{\mathbf{h}}_{\mathcal{T}\xi} + \tilde{\Phi} \tilde{\mathbf{h}}_{\mathcal{T}\xi}) \right] \left[\frac{1}{c^2} \tilde{\mathbf{H}}_{\mathcal{T}\mathcal{T}} \quad \frac{1}{c} \tilde{\mathbf{h}}_{\mathcal{T}\xi} \right]^{-1} \left[\frac{1}{c} (\tilde{\mathbf{h}}_{\mathcal{T}\xi}^T \tilde{\Phi}^T + \tilde{\mathbf{h}}_{\mathcal{T}\xi}^T \tilde{\Phi}^T) \right]. \quad (80)$$

Introduce the Schur complement ρ as

$$\rho = h_{\xi\xi} - \frac{1}{c} \tilde{\mathbf{h}}_{\mathcal{T}\xi}^T c^2 \tilde{\mathbf{H}}_{\mathcal{T}\mathcal{T}}^{-1} \frac{1}{c} \tilde{\mathbf{h}}_{\mathcal{T}\xi} = h_{\xi\xi} - \tilde{\mathbf{h}}_{\mathcal{T}\xi}^T \tilde{\mathbf{H}}_{\mathcal{T}\mathcal{T}}^{-1} \tilde{\mathbf{h}}_{\mathcal{T}\xi}. \quad (81)$$

Proceeding on the calculation of $\mathbf{B}_{\mathbf{p}}^{-1}$, it follows that

$$\begin{bmatrix} \frac{1}{c^2} \tilde{\Phi} \tilde{\mathbf{H}}_{\mathcal{T}\mathcal{T}} & \frac{1}{c} (\tilde{\Phi} \tilde{\mathbf{h}}_{\mathcal{T}\xi} + \tilde{\Phi} \tilde{\mathbf{h}}_{\mathcal{T}\xi}) \end{bmatrix} \begin{bmatrix} \frac{1}{c^2} \tilde{\mathbf{H}}_{\mathcal{T}\mathcal{T}} & \frac{1}{c} \tilde{\mathbf{h}}_{\mathcal{T}\xi} \\ \frac{1}{c} \tilde{\mathbf{h}}_{\mathcal{T}\xi}^T & h_{\xi\xi} \end{bmatrix}^{-1} \begin{bmatrix} \frac{1}{c^2} \tilde{\mathbf{H}}_{\mathcal{T}\mathcal{T}} \tilde{\Phi}^T \\ \frac{1}{c} (\tilde{\mathbf{h}}_{\mathcal{T}\xi}^T \tilde{\Phi}^T + \tilde{\mathbf{h}}_{\mathcal{T}\xi}^T \tilde{\Phi}^T) \end{bmatrix} = \frac{1}{c^2} \left(\tilde{\Phi} \tilde{\mathbf{H}}_{\mathcal{T}\mathcal{T}} \tilde{\Phi}^T + \frac{1}{\rho} \tilde{\Phi} \tilde{\mathbf{h}}_{\mathcal{T}\xi} \tilde{\mathbf{h}}_{\mathcal{T}\xi}^T \tilde{\Phi}^T \right), \quad (82)$$

and then

$$\mathbf{B}_{\mathbf{p}}^{-1} = \frac{1}{c^2} \left(\tilde{\Phi} \tilde{\mathbf{H}}_{\mathcal{T}\mathcal{T}} \tilde{\Phi}^T + \tilde{\Phi} \tilde{\mathbf{H}}_{\mathcal{T}\mathcal{T}} \tilde{\Phi}^T \right) - \frac{1}{c^2} \left(\tilde{\Phi} \tilde{\mathbf{H}}_{\mathcal{T}\mathcal{T}} \tilde{\Phi}^T + \frac{1}{\rho} \tilde{\Phi} \tilde{\mathbf{h}}_{\mathcal{T}\xi} \tilde{\mathbf{h}}_{\mathcal{T}\xi}^T \tilde{\Phi}^T \right)$$

$$= \frac{1}{c^2} \tilde{\Phi} \left(\tilde{\mathbf{H}}_{\mathcal{T}\mathcal{T}} - \frac{1}{\rho} \tilde{\mathbf{h}}_{\mathcal{T}\xi} \tilde{\mathbf{h}}_{\mathcal{T}\xi}^T \right) \tilde{\Phi}^T. \quad (83)$$

Since $\mathbf{D}^2(\boldsymbol{\alpha}) = \kappa \xi d_0^\gamma \mathbf{D}^{-\gamma}(\mathbf{d})$ and $\mathbf{D}^{-1}(\boldsymbol{\tau}) = c \mathbf{D}^{-1}(\mathbf{d})$, we have

$$\tilde{\mathbf{H}}_{\mathcal{T}\mathcal{T}} = \kappa \xi d_0^\gamma \text{SNR} (4\bar{\beta}^2 \mathbf{D}^{-\gamma}(\tilde{\mathbf{d}}) + c^2 \gamma^2 \mathbf{D}^{-(\gamma+2)}(\tilde{\mathbf{d}})) \quad (84a)$$

$$\tilde{\mathbf{H}}_{\mathcal{T}\mathcal{T}} = \kappa \xi d_0^\gamma \text{SNR} (4\bar{\beta}^2 \mathbf{D}^{-\gamma}(\bar{\mathbf{d}}) + c^2 \gamma^2 \mathbf{D}^{-(\gamma+2)}(\bar{\mathbf{d}})) \quad (84b)$$

$$\tilde{\mathbf{h}}_{\mathcal{T}\xi} = -\kappa d_0^\gamma \text{SNR} c \gamma \mathbf{D}^{-(\gamma+1)}(\tilde{\mathbf{d}}) \mathbf{1}_M \quad (84c)$$

$$\bar{\mathbf{h}}_{\mathcal{T}\xi} = -\kappa d_0^\gamma \text{SNR} c \gamma \mathbf{D}^{-(\gamma+1)}(\bar{\mathbf{d}}) \mathbf{1}_{B-M} \quad (84d)$$

$$h_{\xi\xi} = \frac{1}{\xi} \kappa d_0^\gamma \text{SNR} \mathbf{1}^T \mathbf{D}^{-\gamma}(\mathbf{d}) \mathbf{1} \quad (84e)$$

where $\mathbf{d} \in \mathbb{R}^{B \times 1}$ can be written as

$$\mathbf{d} = [\tilde{\mathbf{d}}^T \quad \bar{\mathbf{d}}^T]^T. \quad (85)$$

Substituting (84) into (81), it further yields

$$\begin{aligned} \rho &= h_{\xi\xi} - \tilde{\mathbf{h}}_{\mathcal{T}\xi}^T \tilde{\mathbf{H}}_{\mathcal{T}\mathcal{T}}^{-1} \tilde{\mathbf{h}}_{\mathcal{T}\xi} \\ &= \frac{1}{\xi} \kappa d_0^\gamma \text{SNR} \left(\mathbf{1}^T \mathbf{D}^{-\gamma}(\mathbf{d}) \mathbf{1} - \mathbf{1}_M^T \right. \\ &\quad \left. \left(\frac{1}{4\bar{\beta}^2} c^2 \gamma^2 \mathbf{D}^{-(\gamma+2)}(\tilde{\mathbf{d}}) + \mathbf{D}^{-\gamma}(\tilde{\mathbf{d}}) \right) \mathbf{1}_M \right) \\ &= \frac{1}{\xi} \kappa d_0^\gamma \text{SNR} \left(\mathbf{1}_{B-M}^T \mathbf{D}^{-\gamma}(\bar{\mathbf{d}}) \mathbf{1}_{B-M} \right. \\ &\quad \left. - \frac{1}{4\bar{\beta}^2} c^2 \gamma^2 \mathbf{1}_M^T \mathbf{D}^{-(\gamma+2)}(\tilde{\mathbf{d}}) \mathbf{1}_M \right) \\ &= \frac{1}{\xi} \kappa d_0^\gamma \text{SNR} \rho. \end{aligned} \quad (86)$$

Consider $\tilde{\mathbf{H}}_{\mathcal{T}\mathcal{T}} - (1/\rho) \tilde{\mathbf{h}}_{\mathcal{T}\xi} \tilde{\mathbf{h}}_{\mathcal{T}\xi}^T$

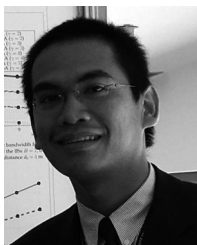
$$\begin{aligned} \tilde{\mathbf{H}}_{\mathcal{T}\mathcal{T}} - \frac{1}{\rho} \tilde{\mathbf{h}}_{\mathcal{T}\xi} \tilde{\mathbf{h}}_{\mathcal{T}\xi}^T &= \kappa d_0^\gamma \text{SNR} \xi \mathbf{D}^{-(1/2)\gamma}(\bar{\mathbf{d}}) (4\bar{\beta}^2 \mathbf{I} + c^2 \gamma^2 \mathbf{D}^{-1}(\bar{\mathbf{d}}) \\ &\quad (\mathbf{I} - \mathbf{D}^{-(1/2)\gamma}(\bar{\mathbf{d}}) \boldsymbol{\Psi}(\rho) \mathbf{D}^{-(1/2)\gamma}(\bar{\mathbf{d}})) \mathbf{D}^{-1}(\bar{\mathbf{d}}) \mathbf{D}^{-(1/2)\gamma}(\bar{\mathbf{d}}) \\ &= 4\kappa d_0^\gamma \text{SNR} \bar{\beta}^2 \xi \mathbf{A}(\rho). \end{aligned} \quad (87)$$

Substituting (87) into (83), we obtain (23).

REFERENCES

- [1] J. H. Reed, K. J. Krizman, B. D. Woerner, and T. S. Rappaport, "An overview of the challenges and progress in meeting the E-911 requirement for location service," *IEEE Commun. Mag.*, pp. 30–37, Apr. 1998.
- [2] J. J. Caffery and G. L. Stuber, "Overview of radiolocation in CDMA cellular systems," *IEEE Commun. Mag.*, pp. 38–45, Apr. 1998.
- [3] K. Pahlavan, X. Li, and J.-P. Makela, "Indoor geolocation science and technology," *IEEE Commun. Mag.*, pp. 112–118, Feb. 2002.

- [4] F. Gustafsson and F. Gunnarsson, "Mobile positioning using wireless networks," *IEEE Signal Process. Mag.*, vol. 22, no. 4, pp. 41–53, Jul. 2005.
- [5] Y. Qi, H. Kobayashi, and H. Suda, "Analysis of wireless geolocation in a non-line-of-sight environment," *IEEE Trans. Wireless Commun.*, vol. 5, no. 3, pp. 672–681, Mar. 2006.
- [6] Y.-T. Chan, W.-Y. Tsui, H.-C. So, and P. chung Ching, "Time-of-arrival based localization under NLOS conditions," *IEEE Trans. Veh. Technol.*, vol. 55, no. 1, pp. 17–24, Jan. 2006.
- [7] H. Miao, K. Yu, and M. J. Juntti, "Positioning for NLOS propagation: Algorithm derivations and Cramer-Rao bounds," *IEEE Trans. Veh. Technol.*, vol. 56, no. 5, pp. 2568–2580, Sep. 2007.
- [8] H. L. Van Trees, *Detection, Estimation, and Modulation Theory, Part I: Detection, Estimation, and Linear Modulation Theory*. New York: Wiley, 2001.
- [9] B. T. Sieskul, F. Zheng, and T. Kaiser, "A hybrid SS-ToA wireless NLoS geolocation based on path attenuation: ToA estimation and CRB for mobile position estimation," *IEEE Trans. Veh. Technol.*, May 2009, to be published.
- [10] H. Hashemi, "The indoor radio propagation channel," *Proc. IEEE*, vol. 81, no. 7, pp. 943–968, Jul. 1993.
- [11] A. N. D'Andrea, U. Mengali, and R. Reggiannini, "The modified Cramér-Rao bound and its application to synchronization problems," *IEEE Trans. Commun.*, vol. 42, no. 2/3/4, pp. 1391–1399, Feb./Mar./Apr. 1994.
- [12] B. Sklar, *Digital Communications: Fundamentals and Applications*, 2nd ed. Upper Saddle River, NJ: Prentice-Hall, 2001.
- [13] V. Erceg, L. Greenstein, S. Tjandra, S. Parkoff, A. Gupta, B. Kulic, A. Julius, and R. Bianchi, "An empirically based path loss model for wireless channels in suburban environments," *IEEE J. Sel. Areas Commun.*, vol. 17, no. 7, pp. 1205–1211, Jul. 1999.
- [14] C. Ma, R. Klukas, and G. Lachapelle, "A nonline-of-sight error-mitigation method for TOA measurements," *IEEE Trans. Veh. Technol.*, vol. 56, pp. 641–651, Mar. 2007.
- [15] S. Stein, "Algorithms for ambiguity function processing," *IEEE Trans. Acoust., Speech, Signal Process.*, vol. 29, no. 3, pp. 588–599, Jun. 1981.
- [16] S. M. Kay, *Fundamentals of Statistical Signal Processing: Estimation Theory*. Englewood Cliffs, NJ: Prentice-Hall, 1993.
- [17] C. C. Craig, "On the frequency function of xy ," *Ann. Math. Stat.*, vol. 7, no. 1, pp. 1–15, Mar. 1936.
- [18] F. Gini and R. Reggiannini, "On the use of Cramér-Rao-like bounds in the presence of random nuisance parameters," *IEEE Trans. Commun.*, vol. 48, no. 12, pp. 2120–2126, Dec. 2000.
- [19] H. L. Van Trees, *Optimum Array Processing. Part IV of Detection, Estimation, and Modulation Theory*. New York: Wiley, 2002.
- [20] P. Tichavský, C. Muravchik, and A. Nehorai, "Posterior Cramér-Rao bounds for discrete-time nonlinear filtering," *IEEE Trans. Signal Process.*, vol. 46, no. 5, pp. 1386–1396, May 1998.
- [21] T. Papaioannou and K. Ferentinos, "On two forms of Fisher's measure of information," *Commun. Stat.—Theory Methods*, vol. 34, no. 7, pp. 1461–1470, Jul. 2005.
- [22] Y. Qi, "Wireless geolocation in a non-line-of-sight environment," Ph.D. dissertation, Princeton Univ., Princeton, NJ, 2003.
- [23] Y. Qi, H. Kobayashi, and H. Suda, "On time-of-arrival positioning in a multipath environment," *IEEE Trans. Veh. Technol.*, vol. 55, no. 5, pp. 1516–1526, Sep. 2006.
- [24] C. D. Meyer, *Matrix analysis and applied linear algebra* Society for Industrial and Applied Mathematics (SIAM), Philadelphia, PA, 2000 [Online]. Available: <http://matrixanalysis.com/>



Bamrung Tau Sieskul (S'05) was born in Lopburi, Thailand, in 1979. He received the B.Eng. and M.Eng. in electrical engineering from Chulalongkorn University, Bangkok, Thailand, in 2002 and 2004, respectively.

In April and May in 2001, he was a summer intern in IBM Thailand Company, Ltd., Bangkok, Thailand. From 2002 to 2004, he was a Research Assistant in the Department of Electrical Engineering, Chulalongkorn University, Bangkok, Thailand. From 2005 to 2006, he was a Scientific Assistant in the

Department of Communication Engineering, University of Duisburg-Essen,

Duisburg, Germany. In 2006, he joined the Institute of Communications Technology, Leibniz University of Hannover, Hanover, Germany, where he is working under Prof. Dr.-Ing. Thomas Kaiser's supervision toward the doctoral degree in electrical engineering. His interests began with direction-of-arrival estimation, antenna array, and linear algebra. Currently, his research lies in the area of signal processing for wireless communications, including estimation bound, multiantenna, channel modeling, channel capacity, and ultrawideband.

Mr. Tau Sieskul published some articles in conference proceedings, journals, and book chapter. He regularly serves as a reviewer for the conferences and journals. He was listed in the *Marquis Who's Who in the World* in 2007.



Feng Zheng (SM'06) received the B.Sc. and M.Sc. degrees in 1984 and 1987, respectively, both in electrical engineering, from Xidian University, Xi'an, China, and the Ph.D. degree in automatic control from Beijing University of Aeronautics and Astronautics, Beijing, China, in 1993.

In the past years, he held an Alexander-von-Humboldt Research Fellowship at the University of Duisburg and research positions at Tsinghua University, National University of Singapore, and University of Limerick, respectively. From 1995 to 1998 he was

with the Center for Space Science and Applied Research, Chinese Academy of Sciences, as an Associate Professor. Since July 2007, he has been with Institute of Communications Technology, Leibniz University of Hannover, as a Wissenschaftlicher Beirat. His research interests are in the areas of UWB-MIMO wireless communications, signal processing, and systems and control theory.

Dr. Zheng is a corecipient of several awards, including the National Natural Science Award in 1999 from the Chinese government, the Science and Technology Achievement Award in 1997 from the State Education Commission of China, and the SICE Best Paper Award in 1994 from the Society of Instrument and Control Engineering of Japan at the Thirty-Third SICE Annual Conference, Tokyo, Japan.



Thomas Kaiser (SM'04) received the Diploma degree from Ruhr-University Bochum, Germany, in 1991 and the Ph.D. (with distinction) and Habilitation degrees from Gerhard-Mercator-University, Duisburg, Germany, in 1995 and 2000, respectively, all in electrical engineering.

From 1995 to 1996, he was on research leave at the University of Southern California, Los Angeles, supported by the German Academic Exchange Service. From April 2000 to March 2001, he was Head of the Department of Communication Systems, Ger-

hard-Mercator-University. From April 2001 to March 2002, he was Head of the Department of Wireless Chips and Systems, Fraunhofer Institute of Microelectronic Circuits and Systems, Germany. From April 2002 to July 2006, he was Coleader of the Smart Antenna Research Team, University of Duisburg-Essen. In summer 2005, he joined the Smart Antenna Research Group, Stanford University; and in winter 2007 Princeton's Electrical Engineering Department as a Visiting Professor. Currently, he chairs the Communication Systems Group, Leibniz University of Hannover, Germany. He is Founder and CEO of mimoOn GmbH. He has published more than 100 papers in international journals and at conferences. His current research interest focuses on applied signal processing with emphasis on multiantenna systems, especially its applicability to ultra-wide-band systems and on implementation issues.

Dr. Kaiser was Guest Editor of several special issues and is coeditor of four books on multiantenna and ultra-wide-band systems. He served on the Editorial Board of the *EURASIP Journal of Applied Signal Processing*. He is involved in several national and international projects, has chaired and cochaired a number of special sessions on multiantenna implementation issues, and is a Technical Program Committee member of several conferences. He was Founding Editor-in-Chief of the IEEE Signal Processing Society e-letter and is Member-At-Large of the Board of Governors of the same society. He was General Chair of the IEEE International Conference on Ultra Wideband 2008 and General Chair of the International Conference on Cognitive Radio Oriented Wireless Networks and Communications 2009.